

Silje Thorstad

Experimental assessment of the oxidation inhibitor KI on fresh and pre-used amines.

Master's thesis in Chemical Engineering

Supervisor: Hanna Knuutila

Co-supervisor: Vanja Buvik

June 2021

Silje Thorstad

Experimental assessment of the oxidation inhibitor KI on fresh and pre-used amines.

Master's thesis in Chemical Engineering
Supervisor: Hanna Knuutila
Co-supervisor: Vanja Buvik
June 2021

Norwegian University of Science and Technology
Faculty of Natural Sciences
Department of Chemical Engineering



Norwegian University of
Science and Technology

Abstract

The increase in the global surface temperature is a serious worldwide problem which could result in catastrophic consequences. Anthropogenic carbon dioxide (CO₂) emissions from power plants using fossil fuels are one of the largest contributors to this increase in global warming. Thus, it has become increasingly important to prevent CO₂ emissions. Post combustion removal of CO₂ by absorption with aqueous amines is one of the ways to reduce these emissions. It is a well-proven commercial technology and have been the most used alternative for over 60 years when it comes to CO₂ removal from natural gas and refinery gases. However, one of the main problems associated with this technology is the amines tendency to degrade, resulting in loss of solvent and corrosion of equipment, thereby yielding a higher operating cost for the plant. Thus, to reduce costs and increase the feasibility of CO₂ capture technologies finding a suitable inhibitor for oxidative degradation in aqueous amine solvents is crucial.

This work presents an experimental study on the oxidative inhibition effect of 2 wt% potassium iodide (KI) in pre-degraded MEA solutions from two different pilot plants, the primary amines 3-amino-1-propanol (AP) and 2-(2-Aminoethoxy)ethanol (DGA) and the inhibition effect of 0.5 wt% KI in aqueous 30 wt% MEA. The experiments were conducted in an oxidative degradation setup consisting of open water bath heated reactors under oxidative conditions consisting of a continuous gas flow of 98% oxygen and 2% CO₂, continuous agitation by magnetic stirring, experimental temperature of 60°C and a loading of 0.4 mol CO₂/mol MEA. The experiments were run for a duration of three weeks and samples of the liquid phase were taken on regular intervals. Various analytical methods were used to determine the amine loss, degradation compounds formed and viscosity.

From the results presented in this thesis KI seems to be a promising oxidative degradation inhibitor for post-combustion CO₂ capture. It is showed that the addition of 2 wt% KI reduces the oxidative degradation significantly for the pre-degraded MEA from pilot scale CO₂ capture and the 30 wt% DGA and 30 wt% AP solutions. This suggests that the inhibition effect of KI is not defeated by degradation compounds already present in the solution and that the effect is independent of primary amine structure. Furthermore, the solution containing 0.5 wt% KI in 30 wt% MEA showed the same inhibiting effect as 30 wt% MEA with 2 wt% KI. The addition of KI did not change the viscosity of the initial pilot solution.

It was detected 11 known degradation compounds in the two different pre-degraded pilot solutions. Here it was shown that the addition of KI reduced the formation rate of some of these compounds. The major degradation compounds detected in the initial pilot solutions were HEPO and HeGly, and after three weeks of further experiments under oxidative conditions the major degradation compounds detected were HEI and HEF.

In all the experiments it was observed a stable amine loss during the 21 days, suggesting that iodide is not consumed while inhibiting the oxidative degradation reactions. The mechanism for which KI inhibits the oxidative degradation is still unclear, but from the results it is suggested that KI salts out the metal from the solution, due to a red precipitate accumulated on the reactor walls was observed which has not been observed without the addition of KI. However, longer oxidative experiments than three weeks should be executed to see if salt depletion will occur. Also, further studies in pilots and cyclic systems are required to assess KI's applicability.

Sammendrag

Økningen i den globale overflatetemperaturen er et alvorlig verdensomspennende problem som kan føre til katastrofale konsekvenser. Antropogene karbondioksid (CO_2) utslipp fra kraftverk som bruker fossilt drivstoff er en av de største bidragsyterne til denne økningen i global oppvarming. Dermed har det blitt stadig viktigere å forhindre disse CO_2 -utslippene. Fjerning av CO_2 etter forbrenning ved absorpsjon med vandige aminer er en av måtene å redusere disse utslippene. Det er en velprøvd kommersiell teknologi og har vært det mest brukte alternativet i over 60 år når det gjelder fjerning av CO_2 fra naturgass og raffineri gasser. Imidlertid er et av hovedproblemene knyttet til denne teknologien aminenes tendens til å brytes ned, noe som resulterer i tap av aminet og korrosjon av utstyr, og dermed gir anlegget en høyere driftskostnad. Derfor er det avgjørende å redusere kostnadene og øke gjennomførbarheten av CO_2 -fangst teknologier ved å finne en passende inhibitor for oksidativ nedbrytning i vandige aminløsninger.

Dette arbeidet presenterer en eksperimentell studie angående den oksidative inhiberingseffekten til 2 vekt% kaliumjodid (KI) i allerede degraderte MEA-løsninger fra to forskjellige pilotanlegg, de primære aminene 3-amino-1-propanol (AP) og 2-(2-Aminoetoksy)etanol (DGA) og inhiberingseffekten av 0.5 vekt% KI i vandig 30 vekt% MEA. Eksperimentene ble utført i et oksidativt nedbrytningsoppsett bestående av vannbad oppvarmede reaktorer under oksidative forhold bestående av en kontinuerlig gasstrøm på 98% oksygen og 2% CO_2 , kontinuerlig røring ved bruk en magnetisk rører, eksperimentell temperatur på 60 °C og en loading på 0,4 mol CO_2 / mol MEA. Eksperimentene varte i tre uker, og prøver av væskefasen ble tatt med jevne mellomrom. Forskjellige analysemetoder ble anvendt for å bestemme tapet av amin, dannede nedbrytningsforbindelser og viskositet.

Fra resultatene presentert i denne oppgaven virker KI som en lovende oksidativ nedbrytningsinhibitor for CO_2 -fangst etter forbrenning. Det ble vist at tilsetningen av 2 vekt% KI reduserer oksidativ nedbrytning betydelig for de to allerede degraderte MEA løsningene fra pilotskala og for 30 vekt% DGA og 30 vekt% AP. Dette antyder at inhiberingseffekten av KI ikke blir beseiret av nedbrytningsforbindelser som allerede er til stede i løsningen, og at effekten er uavhengig av primær aminstruktur. Videre viste løsningen med 0.5 vekt% KI i 30 vekt% MEA den samme inhiberende effekten som 30 vekt% MEA med 2 vekt% KI. Tilsetningen av KI endret ikke viskositeten til startløsningen til den ene pilotprøven.

Det ble påvist 11 kjente nedbrytningsforbindelser i de to forskjellige pre-nedbrutte pilotløsninger. Her ble det vist at tilsetningen av KI reduserte formasjonshastigheten for noen av disse forbindelsene. De viktigste nedbrytningsforbindelsene som ble oppdaget i startprøven til pilotløsningene var HEPO og HeGly, og etter tre uker med ytterligere eksperimenter under oksidative forhold var de viktigste nedbrytningsforbindelsene HEI og HEF. I alle eksperimentene ble det observert et stabilt tap av amin i løpet av de 21 dagene, noe som tyder på at jodid ikke forbrukes samtidig som det inhiberer de oksidative nedbrytningsreaksjonene.

Mekanismen som KI inhiberer oksidativ nedbrytning med, er fremdeles uklar, men fra resultatene er kan det antydes at KI salter ut metallet fra løsningene, på bakgrunn av et rødt bunnfall akkumulert på reaktorveggene ble observert, som ikke har blitt observert uten tilsetning av KI. Imidlertid bør lengre oksidative eksperimenter enn tre uker utføres for å se om saltuttømming vil forekomme. Videre er det nødvendig med forsøk i piloter og sykliske systemer for å vurdere KIs anvendelighet.

Acknowledgements

This work has been performed at the Department of Chemical engineering at the Norwegian University of Science and Technology (NTNU).

I would like to thank my supervisors Hanna Knuutila and Vanja Buvik for the guidance, support and sharing of their knowledge during this thesis. I really appreciate the time and effort they have used. I would especially like to thank Vanja for her guidance and help with the experimental work conducted for this thesis, which is highly appreciated.

Lastly, I want to thank my friends and family for being supportive and pushing me to finish this degree and thesis.

Table of Content

List of figures	1
List of tables	3
Nomenclature	4
1. Introduction	6
1.1 <i>Background</i>	6
1.1.1 Aqueous amine based post-combustion CO ₂ capture	8
1.1.2 Degradation	9
1.2 <i>Objective of this work</i>	10
1.3 <i>Structure of this thesis</i>	11
2. Literature review	13
2.1 <i>Oxidative degradation</i>	13
2.1.1 Oxidative degradation mechanisms	13
2.1.1.1 Hydrogen abstraction mechanism	13
2.1.1.2 Electron abstraction mechanism	15
2.1.2 Degradation compounds	16
2.1.3 Stability of various primary amines	18
2.2 <i>Inhibitors for oxidative degradation</i>	18
2.2.1 Chelating agents	19
2.2.2 Radical/oxygen scavengers	19
2.2.3 Stable salts	19
2.3 <i>Pilot scale studies</i>	20
3. Material and Methods	22
3.1 <i>Chemicals</i>	22
3.2 <i>Methods</i>	22
3.2.1 Preparation of the 30 wt% aqueous amine solutions	22
3.2.2 Oxidative degradation setup	23
3.2.3 Analytical methods	24
3.2.3.1 Titration of total alkalinity	24
3.2.3.2 Total inorganic carbon and total nitrogen	24
3.2.3.3 Heat stable salts	25
3.2.3.4 LC-MS	26
3.2.3.5 Viscosity measurements	26
4. Results and Discussion	27
4.1 <i>Stability of pre-degraded 30 wt% MEA (aq.) pilot plants samples with and without salt addition</i>	27
4.2 <i>Stability of other primary amines (30 wt%) with and without salt addition</i>	32
4.3 <i>The effect of concentration of KI on 30 wt% MEA (aq.) stability</i>	34
4.4 <i>LC-MS</i>	36
4.5 <i>Viscosity</i>	41
5. Conclusion	44
6. Suggestions for future work	45
7. References	46

Appendix A: Material and Methods

51

Appendix B: Results and Discussion

54

List of figures

Figure 1.1. Analysis of the most dominant CO ₂ emission sources ⁴⁵	6
Figure 1.2. Simplified amine-based chemical absorption CO ₂ capture unit ⁴⁸	9
Figure 2.1. The oxidative degradation of MEA via the hydrogen abstraction mechanism, according to Goff and Rochelle ²¹	14
Figure 2.2. Proposed precursor to hydrogen abstraction mechanism, according to Bedell ⁵	15
Figure 2.3. Oxidative degradation of MEA via the electron abstraction mechanism, according to Chi and Rochelle ²¹	15
Figure 2.4. HEI formation according to Arduengo et al ³	17
Figure 2.5. Formation of amides by reaction between MEA and different carboxylic acids, according to Lepaumier et al ³²	17
Figure 2.6. Formation of amides and HSS according to Gouedard et al ²³	17
Figure 2.7. Formation of HeGly from glyoxylic acid in the presence of formic acid, suggested by Vevelstad et al ⁵²	18
Figure 3.1. Flowsheet of the oxidative degradation setup ⁹	24
Figure 4.1. Amine loss during the oxidative degradation experiments of the pre-degraded MEA samples (30 wt% MEA) compared to 30 wt% MEA, all with and without 2 wt% KI. The data for 30 wt% MEA with and without KI was obtained from Buvik et al ⁹ . The amine concentrations are corrected for water loss and loading, by measuring the CO ₂ concentration and amine concentration from TIC and titration, respectively. All experiments were conducted at 60°C. Error bars represent the standard deviation of the three parallels in each experiment. The diagram is obtained from table B.1-4 and B.11 in appendix B.....	28
Figure 4.2. Change in total HSS concentration from day 0 to 21 for the pre-degraded MEA pilot samples (30 wt% MEA) all with and without the addition of 2 wt% KI. All values have been corrected for water loss and loading, and the experiments with salt addition have been corrected for the addition of KI. The error bar represents the standard deviation of the three parallels in each experiment. The diagram was acquired from table B.8 in appendix B.....	29
Figure 4.3. Amine and total nitrogen loss after three weeks for the pilot plant samples (30 wt% MEA) from pilot A and B. The data was obtained from the TN analysis and titration. All values have been corrected for water loss and loading. The error bars represent the standard deviation of the three parallels from the results of the titration and TN analysis in each experiment. The diagram is obtained from table B.9 in appendix B.....	31
Figure 4.4. Amine loss during the oxidative degradation experiments of 30 wt% AP and DGA compared to 30 wt% MEA, all with and without 2 wt% KI. The data for 30 wt% MEA with and without KI was obtained from Buvik et al ⁹ and the data for 30 wt% AP and DGA without KI was obtained from Buvik et al ⁸ . The amine concentrations are corrected for water loss and loading, by measuring the CO ₂ concentration and amine concentration from TIC and titration, respectively. All experiments were conducted at 60°C. Error bars represent the standard deviation of the three parallels in each experiment. The diagram is obtained from table B.5-6 and B.11 in appendix B.	33
Figure 4.5. Amine loss after 21 days for different concentrations of KI in an aqueous 30 wt% MEA solution. All the experiments were conducted at 60°C The data for the results with 2, 1	

and 0.2 wt% KI and no salt addition was obtained from Buvik et al ⁹. All the data have been corrected for water loss and loading. The error bars represent the standard deviation of the three parallels in each experiment. The figure is obtained from table B.7 and B.11 in appendix B. 35

Figure 4.6. MEA concentration [g/kg] obtained from the LC-MS analysis for the unsalted pre-degraded MEA samples from pilot plant A and B and the salted pilot B solution, for day 0 and 21. All the pilot samples contain 30 wt% MEA in the initial solution. The results are corrected for water loss and loading, and the initial solutions are also corrected for pure samples. The error bars represent the standard deviation of the three parallels in each experiment. The figure is obtained from table B.10 in appendix B. 36

Figure 4.7. Concentration [g/kg] of degradation compounds detected in the LC-MS for the pre-degraded MEA sample from pilot plant B for day 0 and 21. The sample contain 30 wt% MEA in the initial solution. The results are corrected for water loss and loading, and the initial solutions are also corrected for pure samples. The error bars represent the standard deviation of the three parallels in each experiment. The figure is obtained from table B.10 in appendix B. 37

Figure 4.8. Concentration [g/kg] of degradation compounds detected in the LC-MS for the pre-degraded MEA sample from pilot plant B with 2 wt% KI for day 0 and 21. The sample contain 30 wt% MEA in the initial solution. The results are corrected for water loss and loading, and the initial solutions are also corrected for pure samples. The error bars represent the standard deviation of the three parallels in each experiment. The figure is obtained from table B.10 in appendix B. 37

Figure 4.9. Concentration [g/kg] of degradation compounds detected in the LC-MS for the pre-degraded MEA sample from pilot plant A for day 0 and 21. The sample contain 30 wt% MEA in the initial solution. The results are corrected for water loss and loading, and the initial solutions are also corrected for pure samples. The error bars represent the standard deviation of the three parallels in each experiment. The figure is obtained from table B.10 in appendix B. 38

Figure 4.10. Change in viscosity from day 0 to 21 for the pre-degraded MEA samples from pilot B with and without KI. The measurements were conducted at 25°C.. The error bars represent the standard deviation of the three parallels in each experiment. The figure is obtained from table B.14 in appendix B. 41

Figure 4.11. The change in viscosity versus CO₂ loading for the pre-degraded pilot samples from pilot B with and without KI, compared to unsalted 30wt% MEA and 30wt% MEA with 2wt% KI obtained from Amundsen et al ² and Buvik et al ⁹, respectively. All experiments were conducted at 25°C. The figure is obtained from table B.14 in appendix B. 42

List of tables

Table 1.1. Overview over the primary amines tested in this thesis.....	11
Table 1.2. Main oxidative degradation compounds detected from the LC-MS analysis of the pre-degraded MEA pilot samples, including their structure, abbreviation, and CAS number.	12
Table 3.1. Overview of the chemicals used in this thesis, including the vendor, purity stated by vendor, CAS number and molecular weight [g/mol].	22

Nomenclature

Abbreviation/Symbol	Description
α	Loading [mol CO ₂ /mol MEA]
α	Carbon in α -position
β	Carbon in β -position
ASI	Auto sample injector
CAS	Chemical abstract service
CCS	Carbon capture and storage
GC-AED	Gas chromatography-Atomic emission detection
GC-FTIR	Gas chromatography-Fourier transform infrared absorption spectrophotometry
GC-MS	Gas chromatography-Mass spectrometry
GHG	Greenhouse gases
IC	Ion chromatography
IEA	The International Energy Agency
IPCC	Intergovernmental Panel on Climate Change
LC-MS	Liquid chromatography-Mass spectrometry
MFC	Mass flow controller
NDIR	Non-dispersive infrared sensor
ORP	Oxidation-reduction potential
PCC	Post-combustion CO ₂ capture
TIC	Total inorganic carbon
TN	Total nitrogen
wt%	Weight percentage

Chemical abbreviations

AMP	2-amino-2-methylpropanol
AP	3-amino-1-propanol
BHEOX	<i>N, N'</i> -Bis(2-Hydroxyethyl)-oxamide
Br ⁻	Bromide ion
CH ₄	Methane
Cl ⁻	Chloride ion
CO	Carbon monoxide
CO ₂	Carbon dioxide
Cu	Copper
DEA	Diethanolamine
DGA	2-(2-Aminoethoxy)ethanol
DMEA	2-Dimethylaminoethanol
EDTA	Ethylenediaminetetraacetic acid
Fe	Iron
Fe ²⁺	Ferrous ion
Fe ³⁺	Ferric ion
FeSO ₄	Iron ³⁺ sulfate
FeSO ₄ ·H ₂ O	Iron ³⁺ sulfate heptahydrate
H·	Hydrogen radical
H ₂	Hydrogen
H ₂ CO ₃	Carbonic acid

HCO ₃ ⁻	Bicarbonate ion
HEA	<i>N</i> -(2-Hydroxyethyl)-acetimide
HEEDA	<i>N</i> -(2-Hydroxyethyl)ethylenediamine
HEF	<i>N</i> -(2-Hydroxyethyl)-formamide
HeGly	<i>N</i> -(2-Hydroxyethyl)glycine
HEHEAA	<i>N</i> -(2-Hydroxyethyl)-2-[(2-Hydroxyethyl)amino]-acetamide
HEI	<i>N</i> -(2-hydroxyethyl)imidazole
HEIA	<i>N</i> -(2-Hydroxyethyl)imidazolidone
HEPO	4-(2-Hydroxyethyl)-2-piperazinone
H ₂ O	Water
H ₃ PO ₄	Phosphoric acid
H ₂ SO ₄	Sulfuric acid
H ₂ S	Hydrogen sulfide
HSS	Heat stable salts
I ⁻	Iodide ion
KBr	Potassium bromide
KCl	Potassium chloride
KCOOH	Potassium formate
KI	Potassium iodide
KNO ₃	Potassium nitrate
MDEA	<i>N</i> -methyldiethanolamine
MEA	Monoethanolamine
MEA urea	<i>N,N'</i> -Bis-(2-Hydroxyethyl)urea
Mn	Manganese
N ₂	Nitrogen
NaHCO ₃	Sodium bicarbonate
NaOH	Sodium hydroxide
NH ₃	Ammonia
N ₂ O	Nitrous oxide
NO ₂	Nitrogen dioxide
NO _x	Nitrogen oxides
O ₂	Oxygen
OH·	Hydroxide radical
OZD	2-oxazolidinone
SO _x	Sulphur oxides
SO ₂	Sulphur dioxide

1. Introduction

In this chapter a background of how anthropogenic CO₂ emissions contributes to global warming, an overview of large anthropogenic CO₂ emission sources and how these emissions can be reduced through carbon capture and storage are first presented. Afterwards, some theory about the CO₂ capture process using amines as an absorbent is presented. Followed by a short description on how degradation limits the potential of this process. In the end, the objective and structure of this thesis is given.

1.1 Background

The Earth's life cycle and global climate is heavily induced by industrial emissions of greenhouse gases (GHG), such as methane (CH₄), nitrous oxide (N₂O), fluorinated gases and carbon dioxide (CO₂)⁴. The single largest contributor to global greenhouse gas emissions are CO₂ emissions resulting from the combustion of industrial processes and fossil fuels (62% in 2010)^{45, 15}. Coal-fired power plants emits approximately 2 billion tons of CO₂ per year, resulting in them being the most dominant CO₂ emission source on the globe, as presented in figure 1.1⁴⁵. Furthermore, approximately 40% of the globally emitted CO₂ emissions originates from power plants. In addition, from 1970 to 2010 there has been a 10% increase in CO₂ concentration from the burning of fossil fuel⁴. According to the International Energy Agency (IEA.), the global anthropogenic CO₂ emissions in 2019 was 33 gigatons²⁷. There are primarily three CO₂ reservoir in the global carbon cycle, these are terrestrial ecosystems, oceans, and the atmosphere. About 40% of the anthropogenic CO₂ emitted directly to the atmosphere accumulates there, approximately 30% is dissolved into the oceans, and the residue is isolated in biological ecosystems²⁰, resulting in an imbalance in the current carbon cycle²⁴. Although, the use and development of renewable energy sources have been growing in the last decade, it is not able to meet the growing energy demand of the whole world⁴⁵. Consequently, one of the most essential problems the world is facing at the moment is how to prevent the undesirable rise in GHG emissions to the atmosphere, resulting in global warming²⁴.

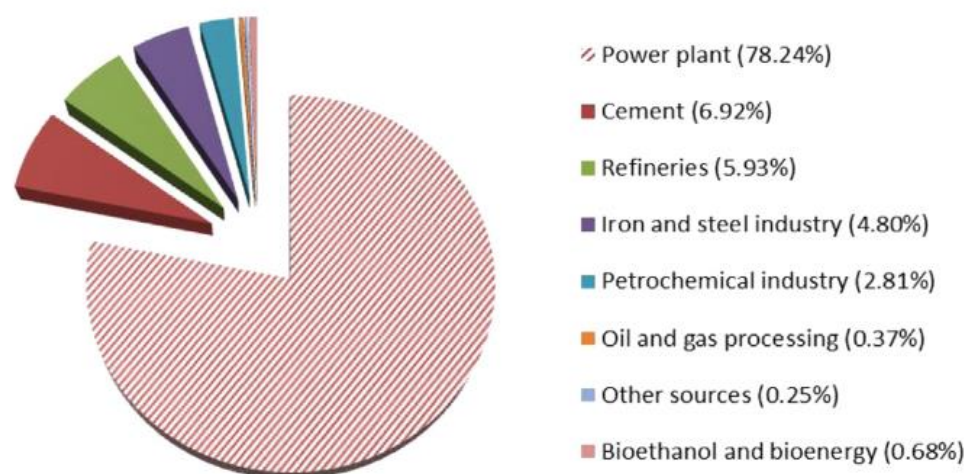


Figure 1.1. Analysis of the most dominant CO₂ emission sources⁴⁵.

The global surface temperature has increased with 0.8°C due to the increase in CO₂ concentrations from 280 to 400 ppm. Lately, it has been measured an alarming level of 408.8 ppm in the CO₂ concentration, resulting from anthropogenic activities⁴. This is

presented by a long-term study at Mauna Loa Observatory, Hawaii, where the atmospheric CO₂ concentration has been measured since 1958, showing that over the last 60 years the CO₂ concentrations have increased by 19%^{20,29}. It is predicted that at the end of this century the CO₂ concentration will increase to 600-700 ppm, yielding an increase in the average surface temperature of 4.5-5°C, if no measures are taken⁴. However, the mean global temperature should not increase by 2°C, according to the Intergovernmental Panel on Climate Change (IPCC.)²⁸, as this would result in a 3.8 m increase in the average sea level. This rise in sea level would cause damage of infrastructure from extreme events, such as increased flooding and salinization of groundwater²⁵. Furthermore, the IPCC predicts that global warming will cause and induce a variety of other harmful effects both globally and on the local environment, such as more extreme weather, reduced agricultural production, less availability of freshwater, ocean acidification and loss of biodiversity^{15, 25}. In addition, indicating effects of global warming has been reported by the IPCC, such as the lowering of the atmosphere, retreat of glaciers and areas with year-round snow coverage is decreasing. The long-term trends in CO₂ concentrations are significantly different from these scenarios²⁰. This is presented in a report by Ruddiman, which is based on the past long-term trends over the last 200 years, presenting that the CO₂ concentrations are significantly higher than what is expected⁴². The National Research Council supports the findings of the IPCC, and agrees that anthropogenic activities are the most probable cause of the accumulating GHG in the atmosphere²⁰.

The IPCC has stated that by 2050 there should be a reduction of 50-80% in GHG emissions, to prevent our planet from a catastrophic collapse. Therefore, at the Conference of Parties-COP 21 in 2015, where 190 countries were present, the main topic was how to control and limit the average temperature rise to 2°C, by limiting the CO₂ concentration by the end of this century. Promotion of energy conservation and efficiency, adapting geoengineering strategies like afforestation, employing renewable and low carbon fuels, and developing carbon capture and storage (CCS) techniques were the recommended strategies from the conference. Hence, a promising and accepted method in reducing the global CO₂ emissions is CCS⁴.

The working principle of CCS is based on at some point in the energy conversion process the CO₂ is separated, followed by compression, transport, and permanent storage. The IEA has stated that by 2050 CCS could provide a reduction of approximately 6 gigatons in CO₂ emissions, if the global temperature is allowed to increase by 2°C at the end of this century. If no measures are taken and a business-as-usual scenario is continued, the CO₂ emissions will increase to 42 gigatons, as an effect of the global temperature increase of 6°C. The global cost of climate change mitigation will be 138% higher, according to the IPCC, if CCS is not undertaken²⁸. Thus, CCS has gained significant attention in recent years as it has the potential to combat global warming by applying fast removal of CO₂ from the atmosphere⁴.

The most representative target for reducing CO₂ emissions are power plants that use fossil fuels, such as natural gas, oil, and coal, as they are large point source emitters, as presented in figure 1.1²⁰. It is estimated that CO₂ emissions in a conventional power plant could be reduced by approximately 80-90% by adding a CO₂ capture and storage unit. Pre-combustion, oxy-fuel combustion and post-combustion capture are the main technologies for CCS^{4 45}.

In pre-combustion capture the CO₂ is captured before combustion and it involves a catalytic reactor and a gasifier⁴. The carbon in the fuel is converted into carbon monoxide (CO) and CO₂ by reacting with oxygen (O₂) and water (H₂O), and simultaneously hydrogen (H₂) is produced. CO is converted into CO₂ after the water gas shift, and the syngas is mainly composed of 20-40% CO₂ and 60-80% H₂⁴⁵. In oxy-fuel combustion a high concentration of CO₂ (over 80%) in the flue gas is produced by combusting the fuel in pure O₂⁴⁵. Post-combustion capture (PCC.)²⁸ is based on CO₂ removal after combustion. This will reduce the emissions from conventional power plants where the fuel is burned with excess air, following emission of the resulting flue gas directly into the atmosphere¹⁵. The concentration of CO₂ in the flue gas is typically 4-14% of the atmospheric pressure. Hence, there is a considerable request to separate the CO₂ in the flue gas and achieve a high CO₂ concentration for storage and transport. This technology can be directly added to existing coal-fired power plants with little retrofitting, compared to oxy-fuel and pre-combustion. For PCC there are several technologies that can be utilized such as absorption, adsorption, membranes, and cryogenics^{45, 4}.

The most cost-effective and viable option based on the available technologies of today is post-combustion removal of CO₂ by absorption with a chemical solvent. Amine-based absorption is a well-proven commercial technology and have been the most used alternative for over 60 years, when it comes to CO₂ removal from natural gas and refinery gases⁴⁸. The method is based on using a liquid amine as an absorbent. The amine solvent absorbs the CO₂ in the flue gas in the absorber by reacting reversibly. The reaction is reversed in the stripper by applying heat to release the captured CO₂²⁰, which can be stored underground or reused³¹. High chemical stability, low vapor pressure and corrosiveness, equilibrium temperature sensitivity, high reaction/absorption rates for CO₂ and high net cyclic capacity are qualities the best absorbents possess. 2-amino-2-methylpropanol (AMP), diethanolamine (DEA), *N*-methyldiethanolamine (MDEA), monoethanolamine (MEA), piperazine and blends of these are the most common studied alkanolamines for PCC⁵¹. The two functional groups in alkanolamines yields an increase in absorption of CO₂ and CO₂ solubility in water, making them widely used as solvents for PCC⁵⁰. Solvent degradation, corrosion and solvent regeneration efficiency are some of the limitations that truly restricts the application of this technology⁴⁵.

1.1.1 Aqueous amine based post-combustion CO₂ capture

Carbamate and bicarbonate formation and carbamate reversion are the chemical reactions taking place in a PCC unit using amine absorbents. The equations for the reactions are given in equation (1), (2) and (3). For primary amines R₁ and R₂ is H and alkyl, and for secondary amines R₁ and R₂ are both alkyls⁵⁰. Equation (1) and (2) are temperature dependent, thus the process can be operated by a temperature swing, where CO₂ is absorbed in the relatively cold amine solvent in the absorber and by application of heat in the stripper the CO₂ is released³⁷.

Figure 1.2 presents a simplified flow diagram of a PCC unit using amines as absorbents. At the bottom of the absorber preconditioned flue gas enters through a blower to increase the pressure. Then, the flue gas and the CO₂ enter the absorber where they react chemically with the counter-current stream of liquid chemical absorbent. This yields formation of equilibrium reactions that produces bicarbonate and carbamate as presented in equation (1), (2) and (3). At the top of the absorber the clean gas, containing mostly nitrogen and oxygen leaves through a washing stage. The washing stage prevents emissions of the absorbent and water-soluble degradation compounds to the atmosphere. From the bottom of the absorber

the CO₂ rich stream proceeds through a cross flow heat exchanger, where it is pre-heated by the stream from the stripper before it is introduced at the top of the stripper. In the stripper the temperature is increased by producing steam from the reboiler, resulting in a reverse in the equilibrium between the CO₂ and absorbent, releasing the captured CO₂. The released CO₂ and water vapor leaves through the top of the stripper, where they pass through a cooler, resulting in water that is re-used in the process and CO₂ that can be compressed and stored. At the bottom of the stripper the lean absorbent is collected before it proceeds through the heat exchanger where it is cooled down, before it enters the absorber and is re-used in the process⁵⁰. Higher molecular weight degradation compounds and heat stable salts (HSS) are removed by a slip stream connected to the stripper and into a reclaiming²¹, to avoid accumulations of these compounds in the circulating solvent²².

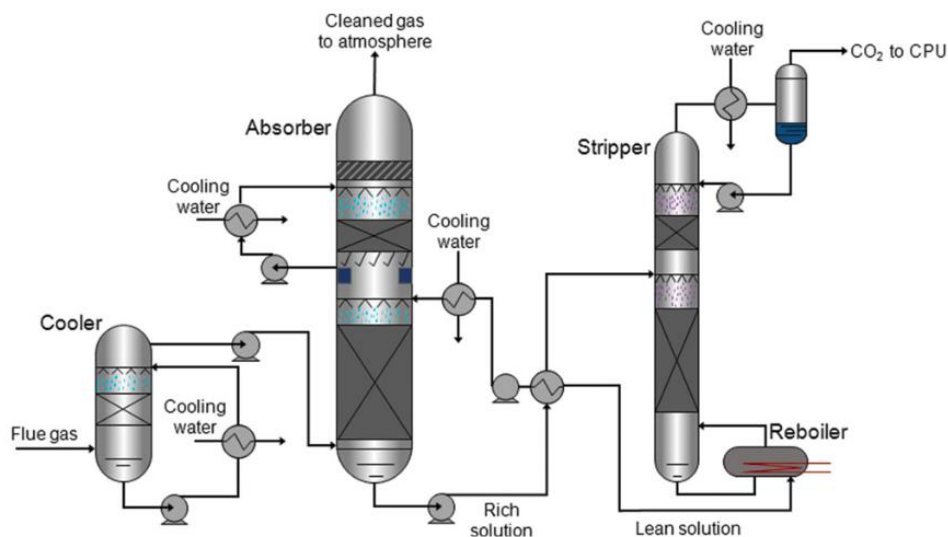
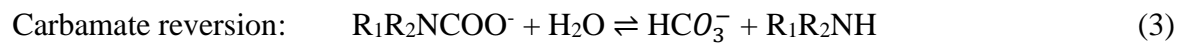
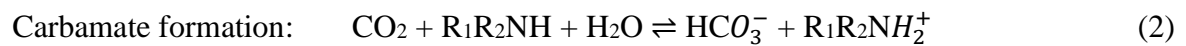
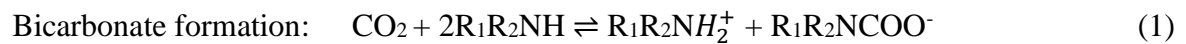


Figure 1.2. Simplified amine-based chemical absorption CO₂ capture unit⁴⁸.

1.1.2 Degradation

One of the main problems associated with large-scale application of amine-based PCC is the amines tendency to degrade through irreversible side reactions with oxygen and CO₂, but also with nitrogen oxides (NO_x) and sulphur oxides (SO_x)¹³. Different problems arise from these reactions, such as foaming, fouling and corrosion, solvent loss and formation of volatile compounds which are potentially dangerous for the environment. Corrosion is a severe problem for acid gas removal systems using alkanolamines. This is presumably caused by the formation of amine carbamates since they are known to be complexing agents. These agents influences the oxygen solubility by changing the properties of the solution, yielding an increase in corrosion and degradation rates^{21, 7}. It has been reported that approximately 10% of the total cost of CO₂ capture is solvent degradation⁴⁹. Thus, it is essential to gain knowledge of amine degradation mechanisms²³.

It is crucial to understand amine degradation as it reduces the plants efficiency to capture CO₂, yielding a higher operational cost and decreased performance of the plant¹⁸. Nevertheless, it is not an easy task to study degradation, mainly due to it being difficult to represent the dynamic cycling system of the solvent in a lab-scale experiment. The solvent is subjected to varying conditions in the real process, leading to various kinds of degradation in different parts of the system. The two main forms of degradation that are expected to occur in a plant is oxidative and thermal degradation. Thermal degradation occurs in the presence of high temperatures and CO₂, therefore it is most likely to occur in the stripper. Oxidative degradation occurs in the presence of oxygen, thus it is most probable to occur where the O₂ concentration is the highest which is the absorber³².

In industrial CO₂ capture applications, the most significant degradation pathway that is experienced for amine loss is oxidative degradation¹¹. Degradation is often the cause for ending a campaign according to experiences from pilot campaigns with MEA¹³. Hence, to reduce the degradation and corrosion in pilot plants various inhibitors have been proposed. Consequently, to reduce costs and increase the feasibility of CO₂ capture technologies finding a suitable inhibitor for oxidative degradation in aqueous amine solvents is crucial⁹.

1.2 Objective of this work

This thesis is a continuation of the work done in the specialization project in the fall of 2020 called “Oxidative Degradation of Monoethanolamine; the effect of increasing temperature, concentration and further use of a degraded sample on the rate of degradation”. The experimental setup, oxidative conditions and experimental procedures used in the project were the exact same as the ones used in this work. The main results from the project showed that increasing the temperature in a 30 wt% MEA solution from 60-80°C increased the rate of oxidative degradation. Thus, more HSS and more nitrogen containing degradation compounds, detected in the TN-analysis, were formed. From the solution containing 50 wt% MEA (tested at 60°C) it was shown that it had the most MEA remaining and less formation of degradation compounds compared to the other experiments in the project. Furthermore, a pre-degraded MEA pilot solution was further tested under oxidative conditions and another solution containing 50% of the pre-degraded MEA pilot sample and 50% fresh MEA (*aq.*) were also tested, both tested at 60°C. The results from these solutions were somewhat strange as they presented that the solution with 50% pilot solvent and 50% fresh MEA (*aq.*) had a higher degradation rate than the fully degraded sample, resulting in more HSS and nitrogen containing degradation compounds formed. This result was suggested to be a result of the degradation compounds already present in the solution further reacting with the fresh MEA in the 50% pilot solution. The further fully degraded pilot solution, called pilot A, was further tested in a LC-MS analysis for this thesis.

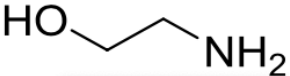
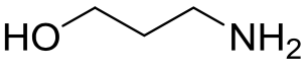
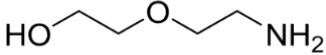
Additionally, this work is also a continuation of the work performed by Buvik et al⁹, on the use of potassium iodide (KI) as an oxidative degradation inhibitor. The main findings of this work will be summed up here briefly. They discovered that addition of KI increases the oxidative stability of MEA significantly. However, it had no effect on the thermal stability, which was equivalent to unsalted MEA. In terms of vapor-liquid equilibrium between CO₂ and the solvent the addition of KI showed little effect. Thus, these factors should not be a concern regarding addition of KI. A further literature review on the oxidative degradation results in this report is given in section 2.2.3.

The objective of this thesis has been to test KI as an oxidative degradation inhibitor in pre-degraded MEA samples from two different pilot plants, to see whether the inhibition effect

of KI on its oxidative stability is defeated by the presence of degradation compounds in the pre-degraded samples. Furthermore, other primary amines than MEA that are known to be unstable under oxidative conditions have been tested, to observe if KI can inhibit other amine structures. The primary amines tested in this work is given in table 1.1. Lastly, 0.5 wt% KI in 30 wt% MEA (*aq.*) was tested to see if inhibition was still achievable.

In correlation with the experimental work executed for this thesis the following chapters will only focus on the oxidative degradation pathways of MEA and the degradation compounds given in table 1.2, as these are the compounds detected in the LC-MS analysis presented in section 3.2.3.4. It will also only focus on MEA based pilot studies.

Table 1.1. Overview over the primary amines tested in this thesis.

Name	Abbreviation	CAS	Structure
Monoethanolamine	MEA	141-43-5	
3-amino-1-propanol	AP	156-87-6	
2-(2-Aminoethoxy)ethanol	DGA	929-06-6	

1.3 Structure of this thesis

Chapter 1 gives an overview of the motivation behind this thesis, regarding global warming and CO₂ capture using aqueous amines. Also, a short description on why degradation limits the use of this technology, and the objective of this thesis are given.

Chapter 2 presents the literature review on the oxidative degradation of MEA, focusing on degradation mechanism and different degradation products formed. Furthermore, the oxidative stability of MEA, AP and DGA, different oxidative degradation inhibitors and main degradation compounds detected in pilot scale were investigated.

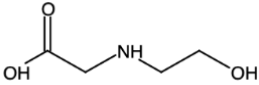
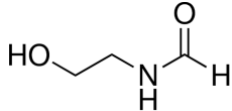
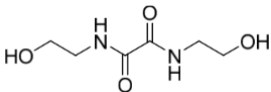
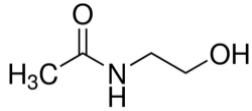
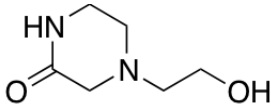
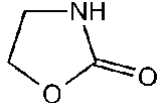
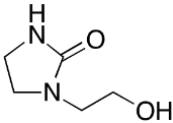
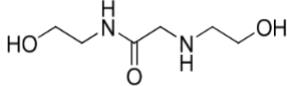
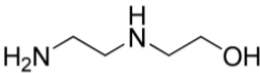
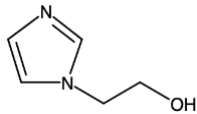
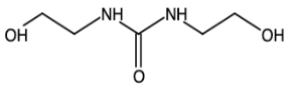
Chapter 3 gives an overview over the chemicals and experimental methods, including the experimental set-up and analytical methods, used in this thesis.

Chapter 4 presents the results from all the experiments conducted in this work. The chapter presents and discuss the inhibiting effect of KI on the oxidative stability of two different pre-degraded MEA pilot samples compared to fresh 30 wt% MEA (*aq.*), the stability of other primary amines compared to 30 wt% MEA (*aq.*) and the effect of the concentration of KI on the oxidative stability of 30 wt% MEA (*aq.*). Moreover, degradation compounds detected in the LC-MS analysis for the pilot samples and viscosity of one of the pilot samples compared to fresh 30 wt% MEA (*aq.*) were presented and discussed.

Chapter 5 presents the conclusion summarizing all the observations from the work executed in this thesis.

Chapter 6 presents suggestions for future work based on the results obtained in this thesis.

Table 1.2. Main oxidative degradation compounds detected from the LC-MS analysis of the pre-degraded MEA pilot samples, including their structure, abbreviation, and CAS number.

Name	Abbreviation	CAS	Structure
<i>N</i>-(2-Hydroxyethyl)glycine	HeGly	5835-28-9	
<i>N</i>-(2-Hydroxyethyl)formamide	HEF	693-06-1	
<i>N,N'</i>-Bis-(2-Hydroxyethyl)oxamide	BHEOX	1871-89-2	
<i>N</i>-(2-Hydroxyethyl)acetamide	HEA	142-26-7	
4-(2-Hydroxyethyl)-2-piperazinone	HEPO	23936-04-1	
2-oxazolidinone	OZD	497-25-6	
<i>N</i>-(2-Hydroxyethyl)imidazolidone	HEIA	3699-54-5	
<i>N</i>-(2-Hydroxyethyl)-2-[(2-hydroxyethyl)amino]-acetamide	HEHEAA	144236-39-5	
<i>N</i>-(2-Hydroxyethyl)ethylenediamine	HEEDA	111-41-1	
<i>N</i>-(2-Hydroxyethyl)imidazole	HEI	1615-14-1	
<i>N,N'</i>-Bis-(2-Hydroxyethyl)urea	MEA urea	15438-70-7	

2. Literature review

In this chapter a literature review on oxidative amine degradation is presented, with a focus on investigating reaction mechanism and different degradation products formed from the solvent monoethanolamine (MEA). The oxidative stability of MEA, 3-amino-1-propanol (AP) and 2-(2-Aminoethoxy)ethanol (DGA) are also investigated and presented along with a study of different oxidative degradation inhibitors. In the end an investigation of the main degradation compounds detected in pilot scale studies compared to lab scale experiments is presented.

2.1 Oxidative degradation

MEA was, until recently, considered a benchmark solvent in post-combustion CO₂ capture (PCC) using chemical absorption and because of this, it is the most studied solvent found in literature¹⁶. It is widely used due to its various advantages, including high CO₂ cyclic capacity, high kinetic at low CO₂ partial pressure, high solubility in water, low viscosity, and its low price. However, a substantial disadvantage is the solvents tendency to degrade, limiting a large deployment of this technology⁴³.

Oxidative degradation of amines occurs in the presence of oxygen (O₂). Dissolved metal ions, including iron (Fe), copper (Cu.), and manganese (Mn), are reported by several studies to catalyze oxidative degradation through the formation of free radicals, which initiates the degradation reactions^{31, 22, 21}. No significant degradation have been observed in the absence of dissolve metals²². Oxidative degradation should be minimized for three primarily reasons. First, a significant operating cost is the replacement of the solvent to maintain the CO₂ capture capacity, due to degradation. It has been reported that 22% of the process operational expenses is solvent makeup necessary to compensate for solvent loss³¹. Second, degradation compounds can induce environmental impact if they are released into the atmosphere or from improper disposal. Lastly, the amine solutions are highly corrosive giving corrosion of the equipment²¹. The main source of amine degradation over time is the harsh operating conditions in the plant, which the solvent is subjected to, due to it continuously being circulated and reused. These conditions include the high temperatures in the stripper, construction material and contact time with all flue gas components⁷.

2.1.1 Oxidative degradation mechanisms

The oxidative degradation of PCC alkanolamine solvents is believed to take place through a peroxy intermediate and therefore may be classified to be of the autooxidation type. The degradation could either be initiated by a reaction with oxygen or by concentration of thermal vibration energy onto one bond, followed by a reaction with oxygen at a close rate to the rate of a diffusion-controlled process¹⁷. However, many aspects of the oxidative degradation mechanism of MEA remain unsolved²¹.

In amine oxidation by a one electron oxidant, it is considered that the initial step proceeds either through hydrogen- or electron abstraction mechanism, yielding a α -C or N centered radical and an aminium radical, respectively. The aminium radical cation is transformed into the same α -C or N centered radical by very fast proton transfer¹⁷.

2.1.1.1 Hydrogen abstraction mechanism

Ionization radiation were used in a study by Petryaev et al³⁶ to create initiating radicals like hydroxyl radical (OH \cdot), hydrogen radical (H \cdot), e⁻ to degrade aqueous amine solutions.

Formation of cyclic 5-membered ring structures containing N-H or O-H bonds is the foundation of the proposed reaction scheme. For α, β -aminoalcohols three reaction options are proposed. The first produces an aldehyde and ammonia (NH_3) by hydrogen abstraction from the β -carbon leading to a N-C cleavage. The second forms an imine which hydrolyses to NH_3 and an aldehyde by hydrogen abstraction from the α -carbon. Lastly, a N-C and C-C bond scission is formed by electron abstraction from the N atom, yielding NH_3 and formaldehyde in the case of MEA^{17, 21}. The proposed hydrogen abstraction mechanism for MEA according to Goff and Rochelle is presented in figure 2.1.

Several molecular simulation studies^{55, 1, 6} supports the validity of the cyclic transition state. Therefore, the primary amino degradation product should be NH_3 , according to these studies. Thus, the degradation mechanism of MEA is believed to proceed via hydrogen abstraction from one of the carbons, then electron abstraction from the nitrogen atom, based on the mechanism proposed by Petryaev et al³⁶ and the molecular simulation studies²¹. However, no studies have been performed to verify which of the pathways that dominates the degradation⁵³.

Potential pathways to produce the organic radical and hydrogen mechanism have been proposed by Bedell, through an hydroxyl radical and organo-peroxy radical⁵. This precursor mechanism is shown in figure 2.2.

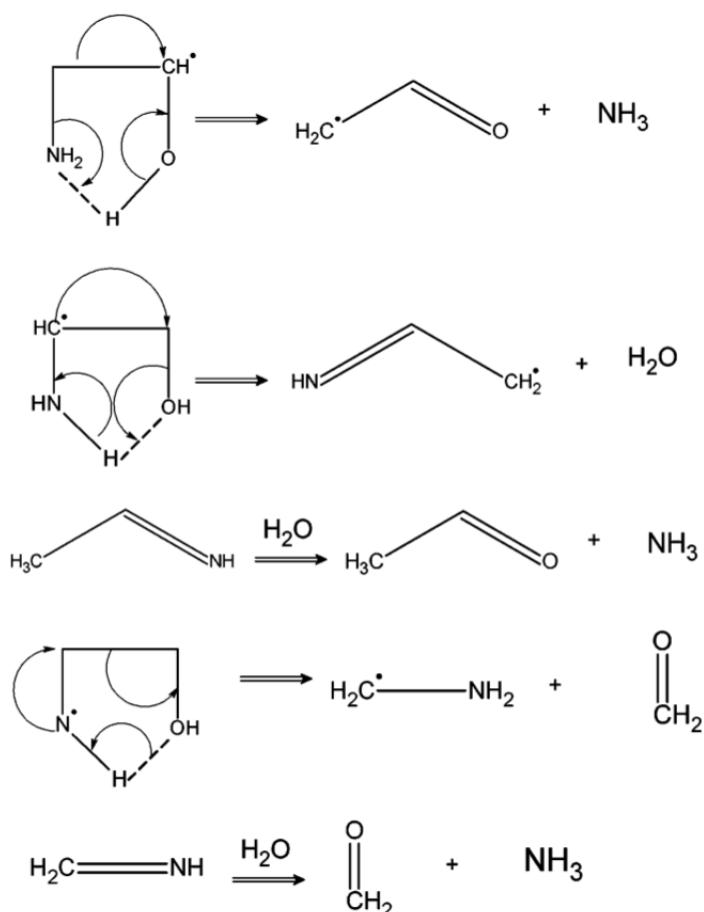


Figure 2.1. The oxidative degradation of MEA via the hydrogen abstraction mechanism, according to Goff and Rochelle²¹.

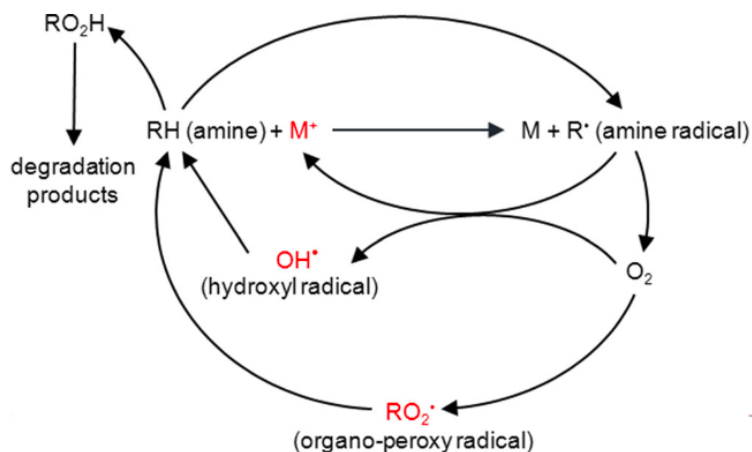


Figure 2.2. Proposed precursor to hydrogen abstraction mechanism, according to Bedell⁵.

2.1.1.2 Electron abstraction mechanism

Studies that mainly focused on using tertiary amines as a single oxidant laid the basis of the electron abstraction mechanism^{40, 12, 26, 41}. These studies suggested that an aminium radical is formed by the electron abstraction from the nitrogen atom, which was indicated to be the rate limiting step. The same aminium radical then produces an imine radical by losing a proton. An imine is produced by further loss of an electron by reaction with another radical. NH_3 together with an aldehyde are produced by hydrolysis of the imine¹⁷.

Chi and Rochelle¹⁰ adopted this mechanism and suggested that this oxidation reaction could be initiated by metal ions such as ferric ion (Fe^{3+}), as presented in figure 2.3. They also proposed to extend the reaction scheme by formation of an amino-peroxide radical from the reaction between oxygen and the imine radical. Then, formation of an amino-peroxide and another aminium radical could occur as a result of the peroxide radical reacting with another molecule of MEA. Hydrogen peroxide and an imine would then be produced by decomposition of the amino peroxide and by reaction with water, an aldehyde and NH_3 are formed²¹.

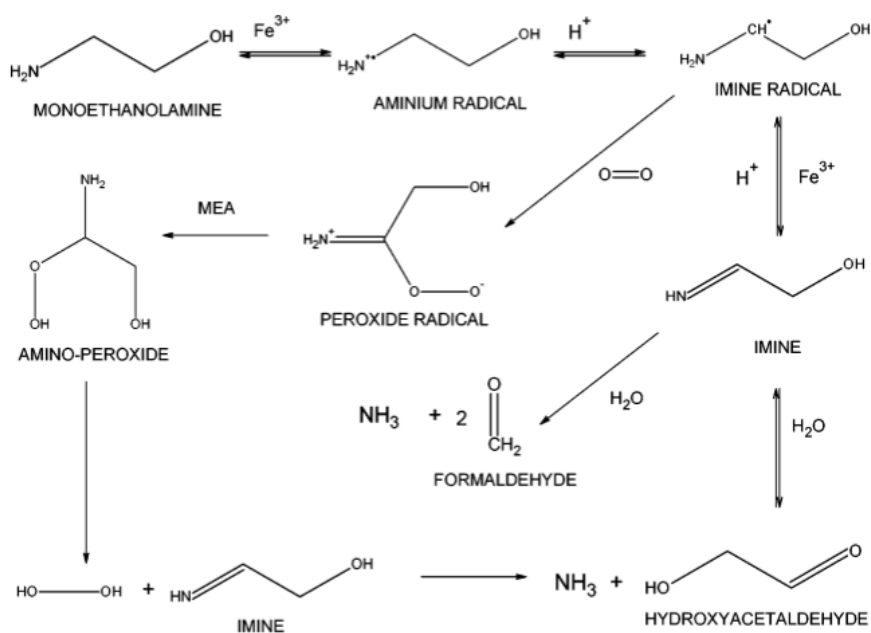


Figure 2.3. Oxidative degradation of MEA via the electron abstraction mechanism, according to Chi and Rochelle²¹.

2.1.2 Degradation compounds

Mechanisms for the formation of identified degradation compounds for MEA have been suggested in the last several years. These mechanisms are based on laboratory scale experiments and pilot samples⁵⁰.

The primary degradation products formed are aldehydes, NH₃, and carboxylic acids. NH₃ and aldehydes are formed by either electron- or hydrogen abstraction mechanisms, and carboxylic acids are formed from oxidation products of some of these compounds⁵¹. Lepaumier et al³³ proposed the formation of carboxylic acids by hydrolyzation of NH₃ and ethylene oxide into ethylene glycol leading to acid formation. Carboxylic acids are formed from rapidly oxidation of aldehydes, even with just air²³.

Reactions between amines and primary degradation compounds forms secondary degradation compounds, such as amides and imidazoles. Imidazoles as *N*-(2-hydroxyethyl)imidazole (HEI) is formed from MEA, NH₃ and various aldehydes. The formation of HEI is given in figure 2.4. Amides as *N*-(2-hydroxyethyl)-formamide (HEF), *N*-(2-hydroxyethyl)-acetamide (HEA) and *N, N'*-Bis(2-hydroxyethyl)-oxamide (BHEOX) are formed from oxygen and aldehyde or MEA and acid⁵¹. These amides are believed to be formed in condensation reactions between amine and the corresponding acid/aldehyde by several studies^{11, 32, 34, 46}, as presented in figure 2.5. Nevertheless, factors influencing the formation of these compounds are still not fully understood⁵¹.

Heat stable salts (HSS) are an important subset of degradation products and includes both covalent and ionic combinations of an acid and an amine. Covalently bonded HSS are formed in a reaction with organic acids, such as carboxylic acids formed from the oxidation of amines, and an amine, as presented in figure 2.6. Ionic HSS are formed from flue gas impurities like sulphur oxides (SO_x) and nitrogen oxides (NO_x). A huge problem associated with HSS is the reduction of CO₂ capacity of the solvent as HSS is not regenerated in the stripper, due to that these compounds can withstand the high temperatures in the process³⁹. Another problem associated with HSS is that they can cause damage to plant construction materials, in case of high concentration buildup, due to their corrosive nature⁴⁷.

N-(2-hydroxyethyl)ethylenediamine (HEEDA) is another degradation compound found in pilot plants. It is proposed to be formed from an ester formation with 2-Dimethylaminoethanol (DMEA) in the presence of carboxylic acids, followed by a ring cyclisation and a S_N2 reaction with another MEA molecule²³. It is proposed two different degradation pathways for the formation of *N*-(2-Hydroxyethyl)-2-[(2-hydroxyethyl)amino]-acetamide (HEHEAA). Da Silva et al¹¹ proposed its formation through a condensation reaction between MEA and *N*-(2-Hydroxyethyl)glycine (HeGly), while Straziar et al⁴⁶ suggested that it was formed through a radical mechanism between MEA and HEA. 2-oxazolidinone (OZD) and 4-(2-Hydroxyethyl)-2-piperazinone (HEPO) are other known degradation compounds and they are proposed to be formed by carbamate ring closure reaction and dehydration of HEHEAA, respectively⁴⁹. Da Silva et al¹¹ suggested that HeGly is a result of a reaction between MEA and a primary degradation compound. However, it was not clear what the precursor was. They also suggest that HEPO is formed in a reaction between MEA and HeGly, first producing the intermediate product HEHEAA through dehydration. Then, HEPO is produced by dehydration of HEHEAA. Vevelstad et al⁵² proposed that HeGly was formed from MEA and glyoxylic acid in the presence of formic acid, as shown in figure 2.7. However, this reaction is proposed to be less favored under basic conditions⁵².

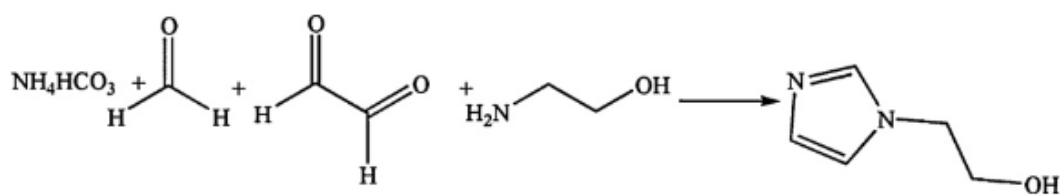


Figure 2.4. HEI formation according to Arduengo et al³.

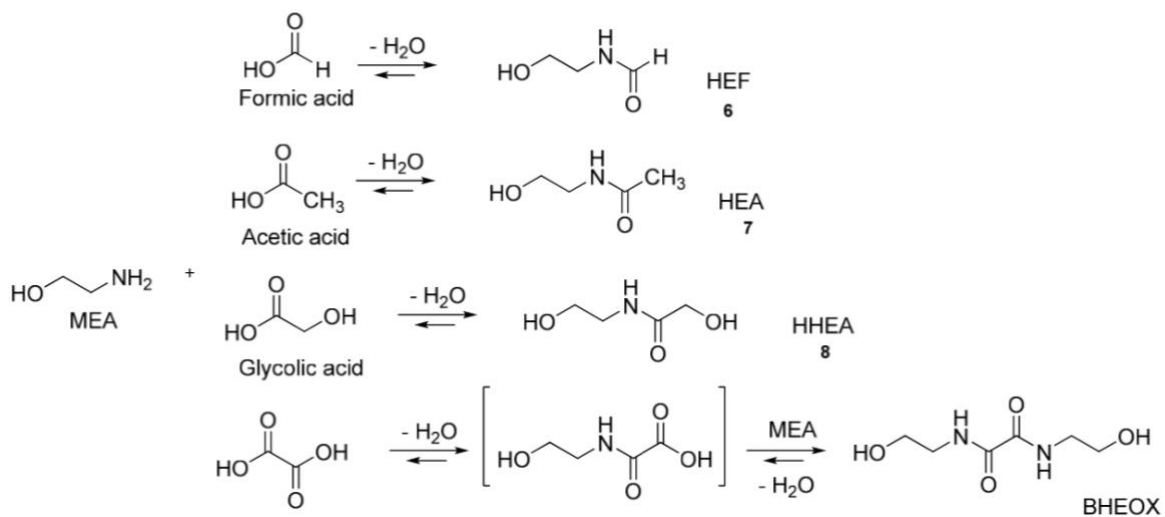


Figure 2.5. Formation of amides by reaction between MEA and different carboxylic acids, according to Lepaumier et al³².

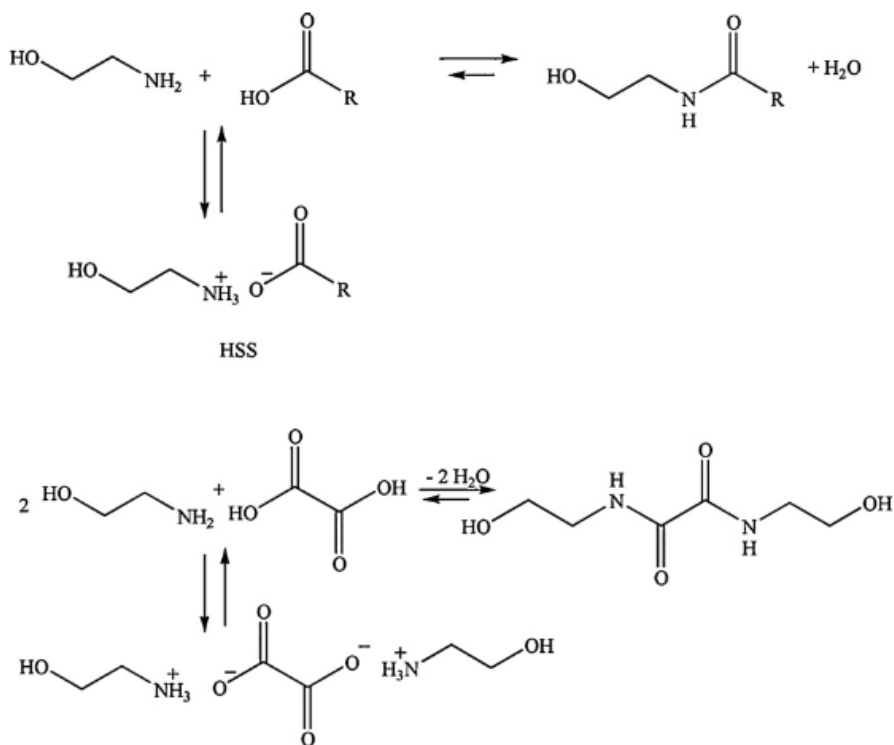


Figure 2.6. Formation of amides and HSS according to Gouedard et al²³.

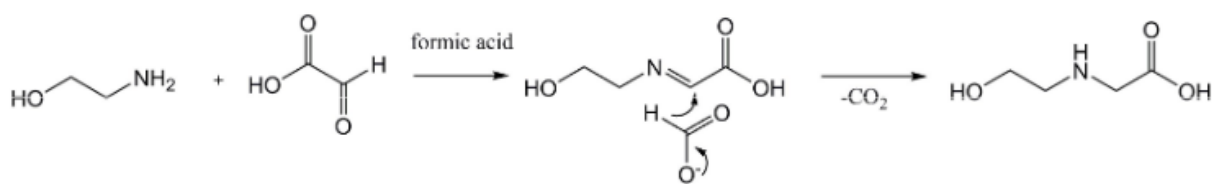


Figure 2.7. Formation of HeGly from glyoxylic acid in the presence of formic acid, suggested by Vevelstad et al⁵².

2.1.3 Stability of various primary amines

During oxidative degradation, type of compounds formed and degradation patterns differ from one amine to another. These reactions depend on the overall process conditions, such as flue gas containing various components, leading to alterations of the stability and degradability of the amine⁸. In correlation with this thesis only information regarding 3-amino-1-propanol (AP), 2-(2-aminoethoxy)ethanol (DGA) and monoethanolamine (MEA) will be reviewed.

Buvik et al⁸ studied eighteen structurally varied amines under harsh oxidative conditions in water bath-heated double-jacketed glass reactors for three weeks (30 wt% amine solution, $\alpha=0.4$, sparged with 98% O₂ and 2% CO₂, 60°C, 0.5 mM iron sulfate) (the exact same reactors that were used in this thesis), to investigate characteristics that can allow a rapid assessment of amine stability under oxidative conditions. The experiments presented that AP and DGA have a higher oxidative stability than MEA, presumably due to steric effects. This result was somehow strange, as both are primary amines that are known, or assumed to form carbamates upon CO₂ absorption, which makes it plausible that their stability should be comparable to that of MEA. In their work, they showed that in the absence of CO₂, MEA displayed a high oxidative stability, indicating that MEA-carbamate may participate in the initiation step of the oxidative degradation reaction. Regardless of the number of substituents on the nitrogen atom, steric hindrance and high substitution can give oxidative stability to amines. The main findings of this work showed that stability of amines is substantially affected by various steric effects, such as bond strain, substituents located both close to and further from the nitrogen atom and chain length. They also suggested that tertiary amines which are known to not form carbamate to a large extent, resulted in them being generally stable. This is in correlation with the findings of Lepaumier et al³⁴ who studied the degradation of 12 different amines under oxidative conditions. They observed that tertiary amines are slightly more stable than primary and secondary amines, due to steric hindrance which prevents dealkylation. Moreover, degradation was reduced due to steric hindrance, resulting in a reduction of formation of highly volatile compounds.

2.2 Inhibitors for oxidative degradation

The rate of O₂ absorption is presumed to control the oxidative degradation of MEA under conditions encountered in a CO₂ capture plant. Therefore, several inhibitors have been proposed in response to degradation mechanisms taking place in the presence of dissolved metals, such as Fe, Cu and Mn, and oxygen. Low cost, nonionic and semivolatile (preferably not removed by ionic or thermal reclaiming), potent at low concentrations (<0.1 wt%), stable at high temperatures and more stable than MEA to oxygen, are ideal qualities of an oxidation inhibitor⁵⁴. Moreover, the efficiency of inhibitors depends on temperature, type of solution, metal surface nature, charge, concentration of inhibitor and molecular structure. In addition, the inhibitor should not cause additional problems to the process, and it should

preferably also inhibit corrosion as well as degradation¹⁸. There are mainly three categories of inhibitors for oxidative degradation, namely, chelating agents, radical/O₂ scavengers and stable salts³¹.

2.2.1 Chelating agents

These inhibitors limit the initiation/propagation steps of the chain reaction by forming a complex with dissolved metals, resulting in inhibition of their catalytic reactivity^{31, 22}. Ethylenediaminetetraacetic acid (EDTA) is a well-known chelating agent, which reduces oxidative degradation by avoiding exposure of Cu and Fe cations to O₂. However, several authors have noticed degradational issues related to EDTA. It has been observed to activate intermediate peroxide and hydroxyl radical formations by promoting Fe formation, thus acting as a catalyst⁴⁹.

2.2.2 Radical/oxygen scavengers

These inhibitors stop the chain reaction by reacting with peroxides to form stable products. The scavenger either reacts with an intermediate in the reaction mechanism or react competitively with O₂ or to react with another free radical. The reaction with O₂/free radicals must be faster than the reaction with MEA^{31, 22}. Leonard et al³¹ proposed that chelating agents are less efficient than radical scavengers. Many radical scavengers must be renewed due to that they are consumed during the reaction, yielding a major disadvantage of these inhibitors^{31, 22}.

2.2.3 Stable salts

These inhibitors reduce the degradation rate by increasing the ionic strength of water, resulting in reduction in the solubility of gases, especially O₂, in the solvent and the rate of absorption. Hence, O₂ is salted out. Potassium chloride (KCl), potassium bromide (KBr) and potassium formate (KCOOH) are examples of stable salt inhibitors^{31, 22}. Application of stable salt yields two significant advantages compared to scavenging additives and toxic inhibitors⁹. That is, their need for replenishment is minimal as they change the properties of the solvent, resulting in that they are not consumed during the degradation reactions. The other is that they are less toxic than for example reactive vanadium or copper salts, which are known degradation inhibitors that are toxic for both humans and the environment¹⁸.

Goff and Rochelle²² tested three stable salts, KCl, KBr and KCOOH in concentrations below 100 mM and above 1.0 M on the oxidative degradation of MEA in the presence of Cu. The results showed that the inhibitors were ineffective at concentrations above 1.0 M. The strongest of the stable salts were potassium formate which reduced degradation of MEA by 15% at 0.55 M. In contrast, Buvik et al⁹ studied the inhibiting effect of the stable salt potassium iodide (KI) on the oxidative degradation of MEA, in the presence of ferrous ion (Fe²⁺). Their results showed KI as a strong oxidative inhibitor, reducing loss of alkalinity after three weeks to 4%, compared to a loss of 40% in a fresh 30 wt% MEA solution. The same inhibiting effect was proven for a solution containing 1 wt% KI (0.06M). They also showed that iodide is not consumed while inhibiting the degradation, since no loss of iodide was discovered during the three weeks using anion exchange chromatography. Furthermore, KI was hypothesized to salt out the metal from the solution, resulting in a more stable solvent under oxidative conditions. The viscosity did not increase significantly for the solution with KI during the three weeks, compared to a fresh MEA solution. In addition, the corrosivity of the solution with KI was comparable to unsalted MEA. However, the cause behind the reduction in degradation due to KI is yet to be properly understood. Furthermore, Lee and Rochelle³⁰ showed that halide containing stable salts

inhibits oxidative degradation of organic acids. Their results presented that, halides react in the increasing order of $\text{Cl}^- < \text{Br}^- < \text{I}^-$ with SO_2 , yielding iodide as the most efficient inhibitor for organic acid degradation. Iodide has also been identified as an effective oxidative degradation inhibitor for organic acids in a recently published patent⁴⁴. In this patent the authors suggested that iodide suppressed the oxidation-reduction potential (ORP) and moderated the sulfite oxidation in the absorber solution. Iodide was also suggested not to be consumed in the process by being oxidized to iodine by reduction of either the catalytically active transition metal ions or the peroxomonosulfate radicals or the sulfite. Excess sulfite could reduce iodine back to iodide. Thus, iodide was proposed to inhibit the overall SO_2 to sulfating reactions⁴⁴.

Research is still ongoing to identify stable oxidative degradation inhibitors for MEA, although previous studies have led to a better understanding of degradation mechanism in the presence of degradation inhibitors and dissolved metals³¹. Nevertheless, some oxidative degradation inhibitors lose their properties in cyclic systems as they are only efficient at absorber conditions and unstable at stripping temperatures⁵⁴.

2.3 Pilot scale studies

Different studies have been conducted to compare degradation compounds detected in laboratory scale experiments with pilot scale. Important information from these findings can be used for the suggestions of different degradation mechanism for the formation of major degradation compounds, and propositions for which degradation pathway is dominant in a pilot plant.

Da Silva et al¹¹ compared MEA degradation experiments in the lab with MEA degradation in three different MEA pilot campaigns, namely a pilot plant at Tiller (Norway), Esbjerg (Denmark) and Longannet (U.K). Samples from the plants were taken from the water wash, the rich MEA solution (high CO_2 content) and the lean solution (low CO_2 content). An open-batch system operated at representative absorber conditions (30 wt% MEA (aq.), $\alpha = 0,4$, sparged with air and CO_2 , 55°C) were used to perform the oxidative degradation experiment, and fly ash or iron (II.) sulfate (FeSO_4) were also added to study its affect. Liquid chromatography combined with mass spectrometry (LC-MS), gas chromatography combined with mass spectrometry (GC-MS) and ion-chromatography (IC) were used to identify and quantify the main degradation compounds from both the pilot plants and the lab experiments. From the analyses it was suggested that oxidative degradation dominates in pilot plants, due to that samples from the pilot plants contained very few degradation products from thermal degradation experiments, compared to oxidative degradation. The dominant degradation products in the pilot plants were HEPO and HeGly, followed by HEA, HEI and HEF as other significant degradation compounds. From the lab-scale experiments the major degradation compounds detected were HEF and HEI. In addition, HEPO, HEA and OZD were also identified. In conclusion, since the solvent is exposed to more varied conditions in pilot plants a wider variety of degradation products are found there than in laboratory experiments.

Lepaumier et al³² compared MEA degradation in the lab with pre-degraded samples from the MEA pilot campaign at the Esbjerg plant (Denmark). An open-batch reactor operated at representative absorber conditions (30 wt% MEA (aq.), $\alpha = 0,4$, sparged with air and CO_2 , 55°C) were used to perform the experiments, to study the effect of CO_2 . LC-MS and GC-MS were used to analyze the samples from both the pilot plant and the lab for amine loss

and identification and quantification of the main degradation compounds, respectively. From the analyses it was suggested that oxidative degradation is the dominant form of degradation in a pilot plant. This being a result of only a few thermal degradation compounds detected compared to detection of all the oxidative degradation compounds in the pilot solvent. Another suggestion of the investigation is that degradation in pilot plants is strongly influenced by the reaction between MEA and carboxylic acids, referred to as heat stable salts, resulting in amide derivatives (HEF, HEA, HHEA, BHEOX). These derivatives could react further to form other complex products (HEPO, HEHEAA). The major oxidative degradation compounds detected in the lab-scale experiments were HEF and HEI, while for the pilot plant the major degradation compounds were HEPO and HEHEAA. The pilot sample contained traces of HEA, HHEA and BHEOX. Furthermore, some degradation products (OZD, HEF and HEI) were detected in both the pilot sample and in the lab-scale experiments. Similarly in this study, it was observed more degradation products in the pilot sample than in the lab-scale experiments.

Stazisar et al⁴⁶ studied solvent degradation in CO₂ capture plants using pre-degraded MEA samples from the IMC Chemical Facility in Trona, California. GC-MS, combined gas chromatography-Fourier transform infrared absorption spectrophotometry (GC-FTIR) and combined gas chromatography-atomic emission detection (GC-AED) were utilized to identify volatile organic compounds in the samples, while inorganic ionic species were identified using IC. OZD and HEIA were observed in trace amounts. HEPO and HEA were also identified. They suggested that HEA is formed due to a reaction between MEA and acetic acid. Similarly in this study, it was observed more degradation compounds in the pilot samples than in lab-scale experiments, indicating that some degradation reactions under plant conditions do not occur in lab-scale experiments. In addition, oxidative degradation was observed to be the significant source of degradation compared to thermal degradation.

3. Material and Methods

This chapter first presents the chemicals, followed by a description of the oxidative experimental setup and experimental procedures used in this work. In the end the analytical methods performed are described and the uncertainty in each method are also given.

3.1 Chemicals

Table 3.1 presents all the chemicals used in this thesis. Two pre-degraded MEA samples from different pilot plants were provided for further use in the oxidative degradation experiment. These samples will be denominated pilot A and B. The sample from pilot plant A contained 1.807 mol CO₂/kg and 3.656 mol amine/kg, and the sample from pilot plant B contained 3.604 mol amine/kg and 0.590 mol CO₂/kg. Deionized water was obtained from a local purification system at NTNU.

Table 3.1. Overview of the chemicals used in this thesis, including the vendor, purity stated by vendor, CAS number and molecular weight [g/mol].

<i>Chemicals</i>	<i>CAS</i>	<i>Molecular weight [g/mol]</i>	<i>Purity stated by vendor</i>	<i>Vendor</i>
<i>Monoethanolamine (MEA)</i>	141-43-5	61.08	>99%	Sigma-Aldrich
<i>Potassium iodide (KI.)</i>	7681-11-0	166.00	>99%	Sigma-Aldrich
<i>Oxygen (O₂)</i>	7782-44-7	32.00	99.999%	AGA
<i>Carbon dioxide (CO₂)</i>	124-38-9	44.01	99.999%	AGA
<i>HIQ SYNTHETIC AIR (21% oxygen in 79% nitrogen)</i>			99.999%	AGA
<i>Iron (II) sulfate heptahydrate (FeSO₄·7H₂O)</i>	7782-63-0	278.01	>99%	Sigma-Aldrich
<i>Ion exchanger Dowex 50W-X8</i>	69011-20-7			Sigma-Aldrich
<i>Degraded MEA solution</i>				Pilot plant A
<i>Degraded MEA solution</i>				Pilot plant B
<i>3-amino-1-propanol (AP)</i>	156-87-6	75.11	99%	Sigma-Aldrich
<i>2-(2-Aminoethoxy)ethanol (DGA)</i>	929-06-6	105.14	98%	Acros Organics

3.2 Methods

The results presented in this thesis contains data reported in earlier work by Buvik et al^{9, 8}, and new data obtained from the experiments performed in this work with pre-degraded MEA pilot samples with and without addition of KI, and addition of KI to aqueous solutions comprising of DGA and AP. All the experiments were conducted using the exact same oxidative degradation setup, operating temperature, loading, gas flow and gas composition and experimental procedures.

3.2.1 Preparation of the 30 wt% aqueous amine solutions

All solutions were prepared gravimetrically, by adding amine (30 wt%) to deionized water on a Mettler Toledo New Classic MS balance, with an accuracy of ± 0.01 g. CO₂ ($\alpha = 0.4$ mol CO₂/mol MEA) was loaded into the aqueous amine solution by bubbling the gas into it, until the desired weight was obtained. Pre-degraded MEA solutions from pilot plants A and B were corrected to contain 30 wt% MEA (assuming all alkalinity of the pre-degraded

solution being MEA) and a loading of 0.4 mol CO₂/mol MEA. KI (2 and 0.5 wt%) and FeSO₄·7H₂O (0.5 mM) were added to the fresh aqueous amine solutions, as well as the corrected pre-degraded pilot solutions, after the addition of CO₂, to inhibit and catalyze the degradation process, respectively. The solutions were stirred with a magnetic stirrer until the FeSO₄·7H₂O and KI had dissolved.

3.2.2 Oxidative degradation setup

The oxidative degradation experiments were run at atmospheric pressure and simulated absorber conditions. A flowsheet of the experimental setup is shown in figure 3.1. Custom made open water bath heated double-jacketed glass reactors (ca. 250 mL) were filled with 200 g of the preloaded aqueous amine solutions (30 wt% (*aq.*) amine, $\alpha = 0,4$ mol CO₂/mol MEA). Each reactor had three openings, one for a gas distribution tube, one for a septum cover to take samples (to not disturb the vapor-liquid equilibrium), and one to attach the condenser. Grease was applied at all openings to minimize vapor loss. Water bath Graham condensers (400 mL) were operated by a VWR cooling bath (5°C), to cool the solution and let out excess gas. A Julabo heating bath was used to heat the reactors. All the experiments were conducted at 60°C. A gas mixture of oxygen and carbon dioxide was continuously distributed into the solution through Pyrex® glass distribution tubes (porosity grade 1) from ALICAT scientific mass flow controllers (MFC), which controlled the gas flow (60 mL/min) and gas composition (2% CO₂, 98% O₂) into the reactors. The gas- composition and flow were based on maintaining a constant loading of 0.4 mol CO₂/mol amine throughout the experiment. Gas wash bottles were used in case of power outage as safety solvent traps between the gas distribution tubes and mass flow controllers. The solutions were under constant stirring (200 rpm) by a magnetic stirring bar during the experimental time using a Stuart SB 161-3 stirring plate.

A hamilton gastight 1005 syringe (5 mL) equipped with a 150 mL stainless steel needle was used to take samples of the liquid phase. The experiments were run for a duration of three weeks, and samples were taken on day 0, 3, 7, 10, 14, 17 and 21. The results presented in this thesis is an average of the three identical parallels each experiment was run in. The uncertainty in each experiment is presented as the standard deviation of the sample average. Uncertainty in each analytical method comes in addition to the standard deviation of the sample average, and the uncertainty is given in the description of each method. The equation for the standard deviation is given in appendix A, Eq (A.3).

All samples were back calculated to the original amine solution at the beginning of the experiment without CO₂, by correcting for evaporation of water and degradation products and loading after three weeks of experiment. It was assumed a linear loss of water throughout the experiment, as the total mass of the solution is only known for the start- and end- solution. Hence, the water loss was calculated from the slope of the trendline of the water loss curve. The equations used to correct for loading and water loss are given in appendix A, Eq. (A.1) and (A.2). The maximum water loss detected after 21 days out of all the experiments performed in this thesis was 7% loss of the initial solution. The CO₂ loadings reported in this thesis were calculated as the ratio between CO₂- and amine concentrations acquired from the TIC- and titration analysis, which are described in section 3.2.3.

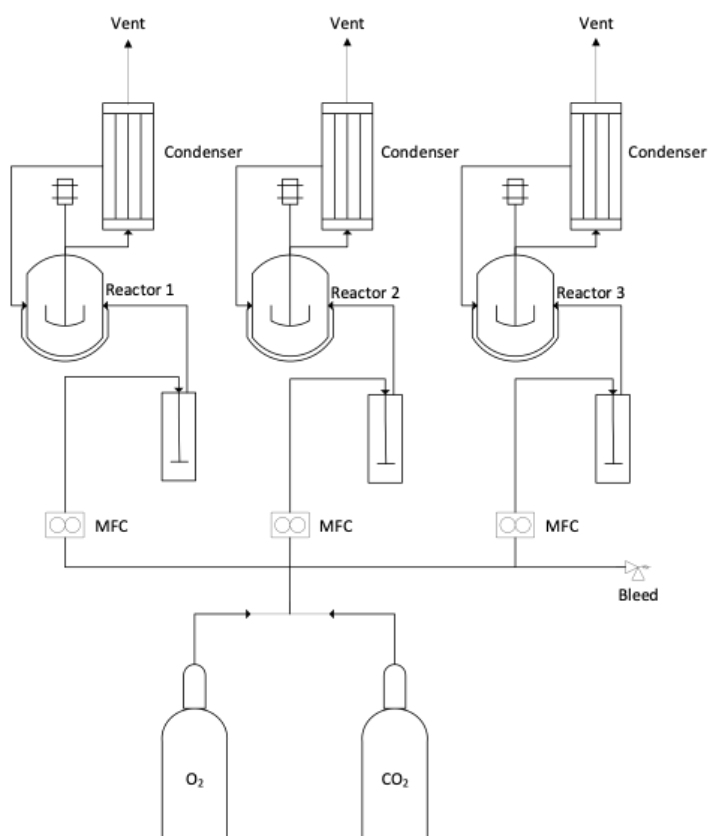


Figure 3.1. Flowsheet of the oxidative degradation setup⁹.

3.2.3 Analytical methods

In the following subchapter all samples were prepared gravimetrically by accurately weighing them on a Mettler Toledo New Classic MS analytical balance, with an accuracy of ± 0.001 g.

3.2.3.1 Titration of total alkalinity

The concentration of amine in the solution was determined by titration on an automatic Mettler Toledo G20 Compact titrator equipped with a Mettler Toledo Rondolino carousel, Mettler Toledo compact stirrer and a Mettler Toledo DGi 115-SC pH electrode. Deionized water (50 mL) was used to dilute the samples (0.2 g), and titration was completed with dilute sulfuric acid (H_2SO_4 , 0.2 N, CAS: 7664-93-9). This method has an uncertainty of $\leq 2\%$ and is in accordance with Ma'mum et al³⁵. Equation (3.1) was used to calculate the concentration of amine in the sample.

$$C_{amine} \left[\frac{\text{mol}}{\text{kg}} \right] = \frac{V_{H_2SO_4} [\text{mL}] * C_{H_2SO_4} [N]}{m_{samples} [g]} \quad (3.1)$$

Where $V_{H_2SO_4}$ is the titration volume [mL], $m_{samples}$ [g] is the amount of amine sample added [g] and $C_{H_2SO_4}$ [N] is the concentration of H_2SO_4 .

3.2.3.2 Total inorganic carbon and total nitrogen

The CO_2 concentration was determined by measuring the total inorganic carbon (TIC) by utilizing a Shimadzu TOC-L_{CPH} equipped with an auto sample injector (ASI). To avoid saturating the detector signal and to achieve a concentration of TIC in the range of 0-500

ppm, the samples (0.4 g) were diluted with purified water (40 mL, 18.2 mΩ) from a Merck Millipore ICW-3000™ water purification system in vials. The instrument was calibrated with sodium bicarbonate (NaHCO₃) before each analysis. The quantification is based on acidifying and sparging the samples into CO₂ and dissolved CO₂ by using 25 wt% phosphoric acid (H₃PO₄) and a carrier gas, respectively. A non-dispersive infrared (NDIR) sensor detects the CO₂ concentration by measuring the amount of infrared radiation of the specific wavelength at which CO₂ absorbs. This method was validated by running it with known standards, and the result were seen valid if the deviation between the concentration measured by the instrument and the known concentration were ≤3%, when used in the range of 10-500 ppm carbon.

A Shimadzu TOC-LCPH equipped with an auto sample injector (ASI) and a TNM-L unit was used to determine the amount of total nitrogen (TN) in the initial- and end solutions. This methods ability to quantify different amines with a universal calibration have shown to be affected by matrix effects, therefore this method was only used to compare the TN content of the start- and end samples. The samples (0.07 g) were diluted with purified water (40 mL, 18.2 mΩ) from a Merck Millipore ICW-3000™ water purification system in vials, to achieve a TN concentration in the range of 0-500 ppm. The instrument was calibrated with potassium nitrate (KNO₃). The quantification is based on oxidative catalytic combustion at 720°C over a platinum catalyst, where the samples decompose to nitrogen monoxide, followed by ozonation into nitrous oxide and excited nitrous oxides. A chemiluminescence detector measures the concentration of nitrogen dioxide, by generating a peak that is proportional to the nitrogen concentration in the sample.

For the experiments with 30 wt% DGA with 2 wt% KI and 30 wt% MEA with 0.5 wt% KI the loading during the time of the experiments were assumed to be equal to the loading obtained for the same compounds without the addition of salt, as presented in Buvik et al⁹. The main cause for this assumption was that at the end of the semester the TIC instrument needed service, thus it was not possible to perform neither a TIC- nor a TN analysis. Another reason is that the exact same oxidative degradation equipment, temperature, gas flow and gas composition were used. Therefore, the concentration of CO₂ in these experiments were calculated from the assumed loading and the results from the titration performed in this thesis. The assumed loading is given in table B.6 and B.7 in appendix B for DGA and MEA, respectively.

3.2.3.3 Heat stable salts

This method was performed according to a method described by Reynolds et al³⁸. A Dowex 50W-X8 ion-exchange resin was used to determine the total concentration of heat stable salts (HSS) in the end (day 21) samples, and for the pilot solutions the start samples (day 0) were also analyzed. The resin (ca. 40 mL) was added to a beaker (250 mL), followed by the addition of deionized water (ca. 40 mL) and the amine sample (ca. 2 g). The samples were partially covered with parafilm and heated (70°C) under magnetic stirring for one hour on a fisherbrand Isotemp heating and stirring plate. After the sample had cooled to room temperature, the supernatant was transferred into a beaker (400 mL) by pouring it through a frit. Deionized water (ca. 40 mL) was added to the resin, followed by stirring of the resin (ca. 1 min), then it was allowed to settle before the supernatant was poured through the frit and into the same beaker as before, to collect all supernatants. Fisherbrand pH-Fix 0.0-6.0 was used to measure the pH of the supernatant. Until the pH of the supernatant was close to the pH of deionized water (pH = 6) the addition of deionized water to the resin was repeated. A 800 Dosino, 801 stirrer equipped with a pH electrode 6.0262.100 from

Metroholm was used to measure the amount of HSS by titrating the collection of all supernatants with diluted sodium hydroxide (NaOH, 0.05 M, CAS: 1310-73-2). Equation (3.2) was used to calculate the total concentration of HSS in the sample.

$$C_{\text{HSS}} = \frac{V_{\text{NaOH}} * C_{\text{NaOH}}}{m_{\text{sample}}} \quad (3.2)$$

Where V_{NaOH} is the volume [mL] of NaOH used to reach the first equivalence point, C_{NaOH} is the concentration of NaOH [M] and m_{sample} is the weight of amine sample [g] added.

This method was validated by running it with a known concentration of HSS in the form of glycolate and acetate in a 30 wt% MEA (*aq.*) solution. From the validation the method showed a maximum uncertainty of $\pm 0,006$ mol HSS/kg (max 6%). The known concentration of HSS and calculated HSS from the titration are given in appendix A in table A.1 and A.2, respectively.

3.2.3.4 LC-MS

Liquid chromatography coupled with mass spectrometry (LC-MS) was utilized to quantify the concentrations of some of the degradation compounds and MEA present in the pre-degraded MEA samples from the pilot plants. The analysis was performed by SINTEF Industry on a UHPLC Agilent 1290 Infinity System with an Agilent 6490 Triple Quadrupole detector. For analyte separation an Ascentis Express PhenylHexyl, 2.7 μm HPLC Column and a Discovery HS F5 HPLC Column were used, both columns were purchased from Sigma-Aldrich Co. LLC. An isotope-labeled internal standard was used to quantify MEA with a typical uncertainty of 3% presented in the results. The raw data from the analysis is given in appendix A table A.3. The pure samples taken directly from the pilot plants were corrected by equation (A.4) in appendix A to the initial pre-degraded 30 wt% MEA solutions used in the experiments in this work.

3.2.3.5 Viscosity measurements

The viscosity of the pre-degraded MEA sample from pilot B with and without the addition of KI were measured using a MCR 100 rheometer from Paar Physica. The measurements were executed at atmospheric pressure and 25°C. Before the analysis a torque calibration was completed to ensure a torque value within $\pm 0.05 \mu\text{Nm}$. Additionally, a measurement of a standard solution of MEA (Viscosity & Density Reference standard, Paragon scientific Ltd, Blend of CAS no.s: 64742-47-8 8042-47-5) was performed, and if the deviation between the viscosity measured and the viscosity given by the ISO 17025 guide were less than <2% the measurements were seen as valid. The sample (ca. 3.6 mL) was injected into the bottom part cylinder and the top part cylinder was lowered to enclose the liquid, ensuring little contact between the surrounding air and the sample. Once the liquid was enclosed the inner cell started rotating in velocities between 10 and 1000 s^{-1} . Shear rate against shear stress was recorded by a computer connected to the instrument, resulting in a line where the slope presented the dynamic viscosity. These samples were not corrected for water loss and loading, since they were compared to literature values for 30 wt% MEA (*aq.*) with loading of 0.4 and 0.5 mol CO_2/mol MEA.

4. Results and Discussion

In this chapter the inhibiting effect of potassium iodide (KI.) on the oxidative stability of both pilot plant samples, A and B, the unstable amines 2-(2-Aminoethoxy)ethanol (DGA) and 3-amino-1-propanol (AP) are presented and discussed. Additionally, the results from the experiment with 0.5 wt% KI in 30 wt% MEA is presented and compared to other concentration of KI in 30 wt% MEA. The results from the LC-MS analysis are presented and compared to other reports focusing on oxidative degradation compounds formed in pilot scale. In the end, the results from the viscosity measurement of pilot B with and without KI are presented and compared to values given in the literature for 30 wt% MEA.

The oxidative degradation of the studied amines presented in this chapter were quantified as the loss of alkalinity throughout the experiment, since this reflects the CO₂ capture efficiency of the solvent. Supporting information regarding degradation mechanism and degradation products formed in the experiments were provided by total nitrogen (TN)-, heat stable salts (HSS)- and LC-MS analysis.

4.1 Stability of pre-degraded 30 wt% MEA (*aq.*) pilot plants samples with and without salt addition

To see whether the inhibition effect of KI on its oxidative stability is defeated by the presence of degradation compounds, it was tested in two different pre-degraded MEA solutions from pilot A and B. The results in this subchapter are compared to the results of 30 wt% MEA with and without the addition of 2 wt% KI, which is presented in a study by Buvik et al ⁹, under the same oxidative conditions and experimental procedures.

The loss of amine during the experimental time of 21 days under oxidative conditions in the pre-degraded MEA samples, compared to a fresh 30 wt% MEA solution with and without 2 wt% KI is presented in figure 4.1. It is observed that addition of 2 wt% KI reduces the amine loss significantly not only for a fresh MEA solution but also for pre-degraded MEA solutions. The addition of KI reduces the loss of amine to $5 \pm 0.3\%$ and $7 \pm 0.3\%$ compared to a loss of $61 \pm 14\%$ and $76 \pm 4\%$ without salt addition for pilot A and B, respectively.

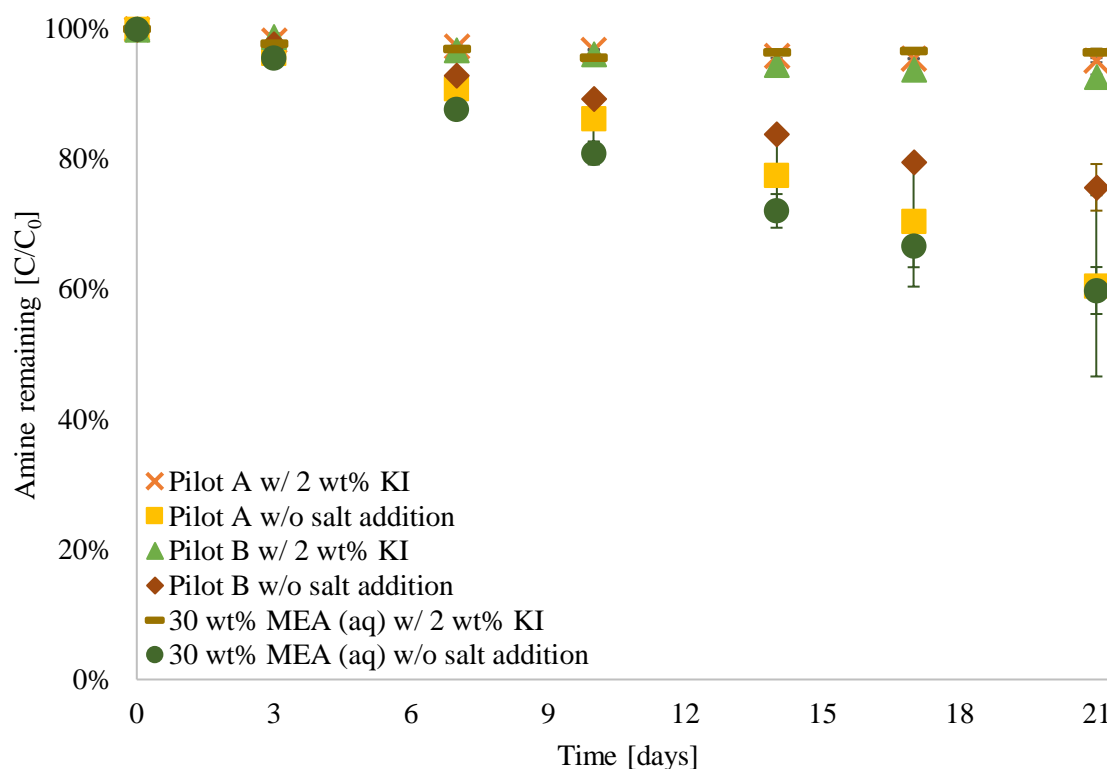


Figure 4.1. Amine loss during the oxidative degradation experiments of the pre-degraded MEA samples (30 wt% MEA) compared to 30 wt% MEA, all with and without 2 wt% KI. The data for 30 wt% MEA with and without KI was obtained from Buvik et al⁹. The amine concentrations are corrected for water loss and loading, by measuring the CO₂ concentration and amine concentration from TIC and titration, respectively. All experiments were conducted at 60°C. Error bars represent the standard deviation of the three parallels in each experiment. The diagram is obtained from table B.1-4 and B.11 in appendix B.

The results presented by the salted pilot solutions are in accordance with the results presented in Buvik et al⁹, where KI reduced the oxidative degradation of MEA. This suggests that the inhibition effect of KI is not defeated by the presence of degradation compounds. The mechanism for which KI inhibits the oxidative degradation is not fully understood⁹. It could be that KI salts out the metal from the solution, resulting in reduced oxidative degradation, as suggested by Buvik et al⁹. Another reason might be that KI prevents the catalytic activity of metal ions in the solution by reacting with them⁴⁴, thus inhibiting the oxidative degradation. Or it might be a result of KI increasing the ionic strength of water, resulting in salting out of the O₂, as explained by Goff and Rochelle²². This will decrease the oxidative degradation since there will be a reduction in dissolved oxygen.

It is also observed that the amine loss for the pilot samples with KI is stable during the 21 days. This suggests that iodide is not consumed during the experiment, as shown in Buvik et al⁹. This could be due to that iodide is oxidized to iodine by reducing either the catalytically active transition metal ions or the peroxomonosulfate radicals or the sulfite. The radicals and sulfite could originate from contaminants in the flue gas. Excess sulfite can reduce iodine back to iodide, thus iodide is not consumed in the process, as suggested by Sjoström et al⁴⁴.

The increase in uncertainty in the unsalted solutions during the three weeks appears to be a result of different oxidative conditions in each parallel, resulting in different degradation rates in each parallel. These conditions could consist of distribution of various gas flows from the gas distribution tubes into the reactors along with different agitation speed in each

reactor, resulting in different bubble sizes which could limit mass transfer from the gas- to liquid phase, giving rise to different degradation rates. Also, if the condensers were not working properly and if fluctuations in temperature in the heating- and cooling bath occurred the reactors would not be properly heated or cooled, resulting in evaporation of water. Thus, different water loss could be experienced in each parallel. This hypothesis is supported by the small uncertainty presented by the salted solutions where the oxidative stability is almost constant, yielding less degradation.

Heat stable salts (HSS) consists of secondary degradation compounds, other salts that can withstand high temperatures and other contaminants from the flue gas present in the pre-degraded pilot solutions. The initial- and end solution of the pre-degraded pilot samples were both tested since they already had been degraded, thus some degradation compounds were present. Moreover, since KI contains a cation, the solutions containing KI were corrected for the addition of this salt due that the method used for determining the amount of HSS utilizes an ion exchanger, hence it will detect KI as HSS. The amount of KI added in each experiment is given in table B.13 in appendix B.

The total HSS concentration in the initial- and end solutions for the pre-degraded pilot samples with and without the addition of KI, is presented in figure 4.2. It is seen an increase in the formation of HSS in the experiments without salt addition compared to the experiments with KI. The addition of salt reduces HSS formation during 21 days to 0.05 ± 0.001 mol/kg and 0.03 ± 0.006 mol/kg compared to a loss of 0.15 ± 0.003 mol/kg and 0.25 ± 0.1 mol/kg for pilot B and A, respectively. Furthermore, unsalted pilot A forms more HSS compared to unsalted pilot B after three weeks.

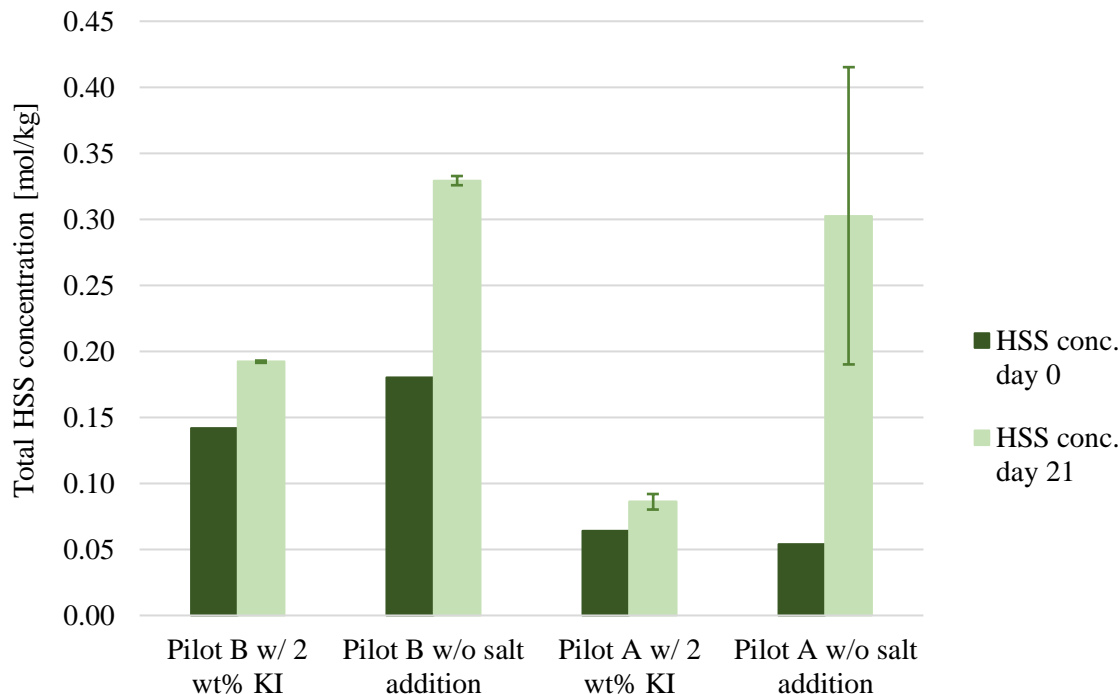


Figure 4.2. Change in total HSS concentration from day 0 to 21 for the pre-degraded MEA pilot samples (30 wt% MEA) all with and without the addition of 2 wt% KI. All values have been corrected for water loss and loading, and the experiments with salt addition have been corrected for the addition of KI. The error bar represents the standard deviation of the three parallels in each experiment. The diagram was acquired from table B.8 in appendix B.

The small increase in HSS concentration for the pilot solutions with KI after three weeks is in accordance with the amine loss presented in figure 4.1, where it is detected a small amine loss after three weeks for the experiments with KI. This is presumably due to the degradation compounds and dissolve metals already present in the pilot solutions. These compounds could react further with the MEA already present and the fresh MEA introduced into the solution⁵¹, which was used to make the initial 30 wt% MEA pilot solutions used in these experiments, resulting in the production of more degradation compounds. The larger increase in HSS concentration after three weeks for the unsalted pilot solutions is expected, as these experiments did not contain an inhibitor. Therefore, oxidative degradation occurs, resulting in formation of degradation compounds. Moreover, it is observed that salted pilot B contains less HSS than the unsalted solution at the start of the experiment. This is somewhat strange as the initial concentration in both pilot B solutions should have been the same, as they were made with the same pre-degraded pilot solution, and the loading and weight percentage of MEA were corrected with the same amount of CO₂ and MEA. The only difference is the addition of KI. This salt does not appear to yield such a large difference as the initial solution for pilot A with and without KI is almost the same. Hence, the difference could be a result of the execution of the method or different operating conditions in each parallel, resulting in different degradation rates. Furthermore, the large uncertainty presented in unsalted pilot A, might reflect the different amine loss in each parallel, as shown in figure 4.1, resulting in different HSS concentrations in the end samples.

The large formation of HSS in unsalted pilot A compared to unsalted pilot B after three weeks is very interesting. This is due to the larger loss of amine in unsalted pilot A compared to unsalted pilot B, as presented in figure 4.1, leading to the formation of more degradation compounds. The precursor for this degradation might be due to the initial concentration of HSS in the initial pre-degraded sample taken directly from the plants, where it is seen that pilot A has a lower HSS concentration at the start than pilot B. It is therefore suggested that the high concentration in unsalted pilot B compared to unsalted pilot A in the initial solution has a positive effect on amine stability. This suggestion is based on that less HSS are formed and the degradation rate in unsalted pilot B is slower than unsalted pilot A after three weeks, as presented in figure 4.1. The reason for the different concentrations might be due to different operating conditions in the pilot plants, resulting in different concentrations of degradation compounds formed, as suggested by da Silva et al¹¹. This could for example be that the pilot plants operate with different flue gases containing various compounds with different concentrations and contaminants. Thus, these compounds/contaminants are transported into the solvents, yielding different concentrations of HSS. However, with these results it is quite difficult to deduce if the HSS concentration in the initial solutions originates from flue gas compounds/contaminants or degradation of the solvent. Nevertheless, the result from the LC-MS analysis of the initial unsalted pilot solutions showed that pilot B contained more degradation compounds than pilot A, as presented in figure 4.7 and 4.9 in section 4.4. Hence, supporting the suggestion that degradation compounds might have a positive effect on amine stability. In addition, it is somewhat strange that unsalted pilot A has the least concentration of HSS to begin with, still it degrades quicker than unsalted pilot B, as shown in figure 4.1. This result is contradictory to the exponential degradation rate observed in pilot scale by Dhingra et al¹³.

The removal of HSS from the solvent in the reclaimer in a CO₂ capture facility might also remove KI, as KI might be detected as a heat stable salt. However, degradation of MEA is heavily reduced by the addition of KI, which implies that the need for reclaiming to keep

the HSS concentration in the solvent low enough would also be reduced. This could make up for the cost of inhibitor replenishment, as less solvent is lost and less HSS needs to be reclaimed. Nevertheless, it is wise to evaluate if KI should be recovered from the reclamation, as it is relatively costly.

Total nitrogen (TN) analysis was used to determine the total nitrogen concentration in the pre-degraded pilot samples both with and without KI after three weeks, compared to day 0. These results were compared to the results from the titration to get an indication of the types of degradation compounds formed, as presented in figure 4.3. Nitrogen lost is assumed to be the same as amine lost and total nitrogen conserved is assumed to be nitrogen containing degradation compounds. It is observed that the addition of KI conserves the amine considerably better, less nitrogen is lost, and less nitrogen containing degradation compounds are formed (total nitrogen conserved) after three weeks, compared to the experiments without salt addition. Unsalted pilot A shows a greater loss in amine- and total nitrogen conservation and loss of nitrogen compared to pilot B without addition of KI. It is noticed that salted pilot A conserves amine and total nitrogen better than salted pilot B. However, salted pilot B has less nitrogen lost than salted pilot A.

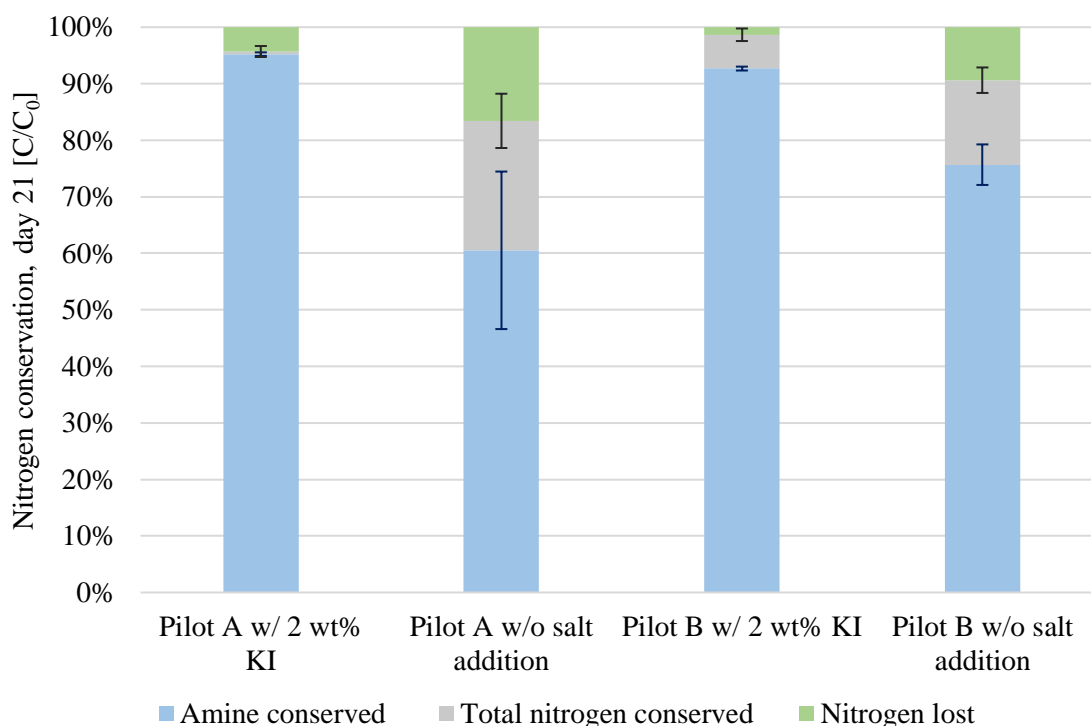


Figure 4.3. Amine and total nitrogen loss after three weeks for the pilot plant samples (30 wt% MEA) from pilot A and B. The data was obtained from the TN analysis and titration. All values have been corrected for water loss and loading. The error bars represent the standard deviation of the three parallels from the results of the titration and TN analysis in each experiment. The diagram is obtained from table B.9 in appendix B.

More volatile nitrogen containing degradation compounds, such as ammonia, is formed in the unsalted pilot solutions compared to the salted solutions, by observing the increase in nitrogen conservation after three weeks. However, the method does not identify which degradation compounds are present, but it allows an assessment of the amount of emissions that can be expected. The nitrogen losses are in accordance with the HSS results presented in figure 4.2 and the amine loss presented in figure 4.1, where the unsalted pilot solutions produce more HSS and have a higher amine loss after three weeks compared to the salted pilot solutions. The differences in amine- and total nitrogen conservation and nitrogen lost

between pilot A and B with KI is very small. This might be explained by the uncertainties in the TN- and titration method, resulting in a too large uncertainty to relate these results to the oxidative degradation taking place. Again, the uncertainty in unsalted pilot A is large, most likely due to various operating conditions in each parallel, resulting in different degradation rates in each parallel.

The results for the TN- and HSS analysis were not compared to HSS- and TN values for 2 wt% KI in 30 wt% MEA, due to the minor amine loss presented in figure 4.1 and the uncertainty in both methods (titration and TN), yielding a too large uncertainty to provide any useful information.

In summary, the results presented in this subchapter clearly shows that the addition of KI reduces the oxidative degradation of amines significantly in both pilot solutions by reducing the formation of HSS and other nitrogen containing degradation compounds after three weeks, compared to the same solutions without salt addition. These results are in accordance with the results presented in Buvik et al⁹ on the oxidative stability of KI as an inhibitor for MEA. This indicates that degradation compounds already present in pre-degraded pilot solutions do not defeat the oxidative inhibiting effect of KI.

4.2 Stability of other primary amines (30 wt%) with and without salt addition

The KI inhibitor was tested with DGA and AP, which are known to be unstable primary amines under oxidative conditions, to see if it could stabilize other amine structures besides MEA. The results presented in this subchapter are compared with results from experiments with DGA and AP, without the addition of salt, reported in Buvik et al⁸, under the same oxidative conditions and experimental procedures.

The loss of amine throughout the experimental time of three weeks under oxidative conditions in aqueous 30 wt% solutions of DGA and AP, compared to a fresh 30 wt% MEA solution with and without 2 wt% KI is presented in figure 4.4. It is observed that addition of 2 wt% KI not only stabilizes MEA, but also DGA and AP. The addition of KI yields a conservation of amine of $100 \pm 1\%$ and $98 \pm 0.2\%$ compared to a loss of $91 \pm 1\%$ and $80 \pm 2\%$ without salt addition for AP and DGA, respectively. AP shows zero loss of amine after three weeks compared to the other two solutions, while MEA presents the highest loss both with and without salt addition.

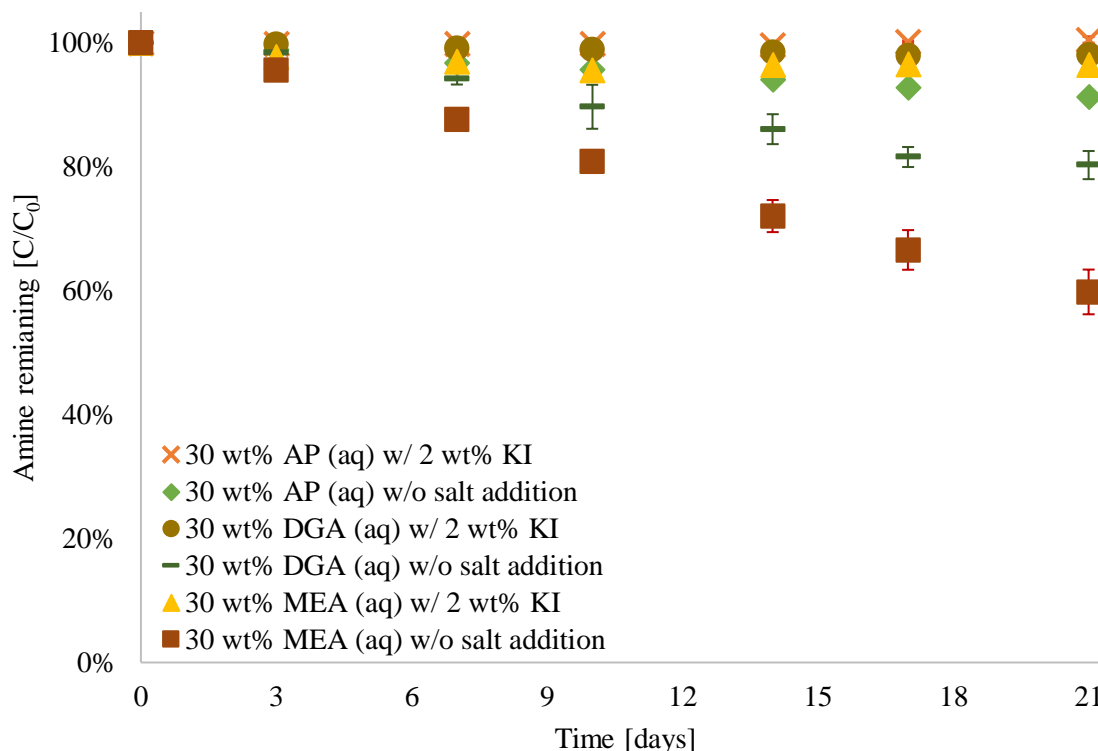


Figure 4.4. Amine loss during the oxidative degradation experiments of 30 wt% AP and DGA compared to 30 wt% MEA, all with and without 2 wt% KI. The data for 30 wt% MEA with and without KI was obtained from Buvik et al⁹ and the data for 30 wt% AP and DGA without KI was obtained from Buvik et al⁸. The amine concentrations are corrected for water loss and loading, by measuring the CO₂ concentration and amine concentration from TIC and titration, respectively. All experiments were conducted at 60°C. Error bars represent the standard deviation of the three parallels in each experiment. The diagram is obtained from table B.5-6 and B.11 in appendix B.

Both AP and DGA presents a higher oxidative stability than MEA both with and without KI. This might be due to the steric effect caused by the extended chain length in AP and DGA compared to MEA, as suggested in Buvik et al⁸, resulting in reduction of formation of degradation compounds. This is supported by the finding by Lepaumier et al³⁴, who also suggested that degradation was reduced due to steric hindrance. These results suggests that the inhibition effect of KI is independent of amine structure, at least for primary amines. During the three weeks of experiments with KI it was observed a red precipitate accumulated on the reactor walls and the typical orange/yellow color of iron-containing solutions were not as distinct as it would have been without the addition of KI. The same observation was made by Buvik et al⁹. It is therefore suggested that KI salts out the metal from the solution, resulting in a more stable solvent under oxidative conditions, supporting the hypothesis regarding the same effect in Buvik et al⁹. Also, in this subchapter the amine loss after three weeks for the solvents with KI is stable, suggesting that iodide is not consumed while inhibiting the reaction⁹. For more discussion regarding how KI may inhibit the oxidative degradation see section 4.1.

Furthermore, it is also observed that the unsalted solutions have a higher uncertainty, except for AP, compared to the salted solutions during the three weeks. Again, this appears to be a result of small variations of the oxidative conditions in each parallel, resulting in slightly different degradation rates in each parallel, as discussed in section 4.1. This is supported by the small uncertainty presented by the salted solutions, where the oxidative stability is almost constant.

It was assumed that the initial concentration of HSS in the initial solution in the experiments with 30 wt% AP and DGA both with 2 wt% KI were neglectable since both solutions contained fresh AP and DGA. Therefore, the start solutions were not tested. The experiments with KI were corrected for the addition of this salt. The amount of KI added in each experiment is given in table B.13 in appendix B.

The results from the HSS analysis presented that the addition of KI did not produce any HSS for DGA or AP compared to the same solutions without salt addition after three weeks with exposure to oxidative conditions. The result for 30 wt% AP and DGA both with 2 wt% KI is given in table B.8 and the result from the unsalted solutions are given in table B.15 in appendix B. This is in accordance with the result presented in figure 4.4, as there is detected almost zero loss of amine after three weeks for the salted solutions, resulting in less formation of degradation compounds. However, the results presented for the salted solutions is somewhat strange as they are negative, when correcting for KI. This might be due to the minor amine loss in figure 4.4 and uncertainty in the method, resulting in a too large uncertainty to provide useful results

The results from the TN analysis also presented that 30 wt% AP with 2 wt% KI did not lose any amine compared to an unsalted solution after three weeks with exposure to oxidative conditions. The results are presented in table B.9 in appendix B. 30 wt% DGA with KI was not tested as explained in section 3.2.3.2. Again, the results are somewhat strange for KI as the value for nitrogen lost is negative. This might be due to the minor amine loss presented in figure 4.4 and the uncertainty in both methods (titration and TN) which yields a too large uncertainty to provide any useful results.

In summary, the results presented in this subchapter clearly shows that the addition of KI yields a higher oxidative stability for AP and DGA compared to MEA by reducing the formation of HSS and other nitrogen containing degradation compounds after three weeks, compared to the same solutions without salt addition. This suggests that the inhibition effect of KI is independent for primary amines. However, it is difficult to draw any conclusions from the TN- and HSS analysis due to the result being somewhat strange, which could be a result of the minor amine loss and the uncertainty in each analytical method.

4.3 The effect of concentration of KI on 30 wt% MEA (aq.) stability

A further investigation to assess the concentration of KI necessary to stabilize aqueous 30 wt% MEA under oxidative conditions was conducted in this thesis with 0.5 wt% KI. From an earlier study reported by Buvik et al⁹ experiments containing 30 wt% MEA with concentrations of 2, 1 and 0.2 wt% KI and no salt addition have been performed, under equal oxidative conditions. The results from this study will be further used and discussed in this subchapter.

The loss of amine throughout the experimental time of three weeks under oxidative conditions for different concentrations of KI in a 30 wt% MEA solution compared to a 30 wt% MEA solution without salt addition is presented in figure 4.5. It is observed that a KI concentration of 0.5 wt% presents the same inhibiting effect as 2 wt% KI. However, reducing the concentration to 0.2 wt% KI reduces the effect significantly.

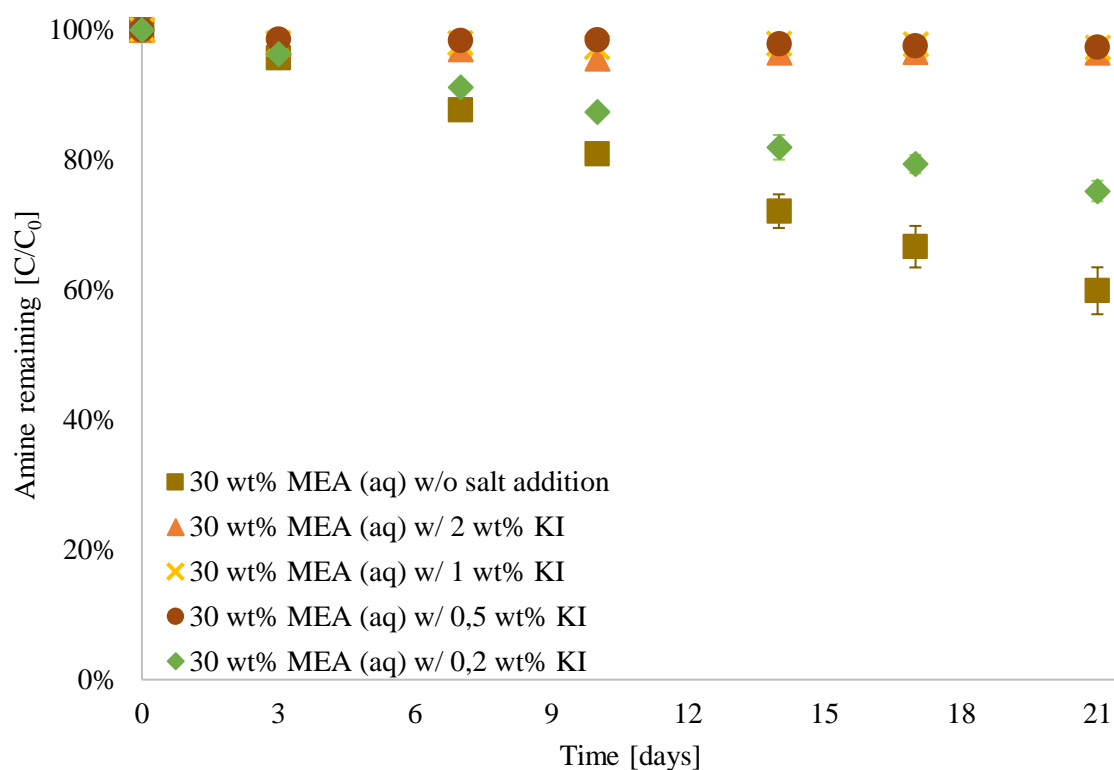


Figure 4.5. Amine loss after 21 days for different concentrations of KI in an aqueous 30 wt% MEA solution. All the experiments were conducted at 60°C. The data for the results with 2, 1 and 0.2 wt% KI and no salt addition was obtained from Buvik et al⁹. All the data have been corrected for water loss and loading. The error bars represent the standard deviation of the three parallels in each experiment. The figure is obtained from table B.7 and B.11 in appendix B.

The inhibiting effect of KI on oxidative degradation is equally strong for 0.5 wt% as for 1 wt% after three weeks. This suggests that even though only 0.5 wt% KI instead of 2 wt% is used, KI is not consumed during the reaction. However, longer oxidative experiments than three weeks should be executed to see if there will be a reduction in stability after three weeks. Furthermore, the results suggests that a concentration between 0.2 and 0.5 wt% is the minimum concentration of KI needed to obtain the same oxidative inhibiting effect. Also, it was observed the same red precipitate accumulation on the reactor wall during the three weeks, as discussed in the previous section, supporting the hypothesis that KI salts out the metal⁹.

The HSS analysis showed no formation of HSS after three weeks of exposure to oxidative conditions for 30 wt% MEA with 0.5 wt% KI, as shown in table B.8 in appendix B. This is in accordance with the conservation of amine in the same solution presented in figure 4.5, resulting in less formation of degradation compounds.

There was not performed a TN analysis for the experiment with 30 wt% MEA with 0.5 wt% KI, as explained in section 3.2.3.2. Even so, based on the results presented in this and the two previous subchapters, it is assumed that the addition of 0.5 wt% KI will probably provide almost the same results as 30 wt% AP with 2 wt% KI, where the value for nitrogen lost is negative. Again, this yields a too large uncertainty to provide any useful results.

In summary, the result in this subchapter shows that the addition of only 0.5 wt% KI in 30 wt% MEA presents the same oxidative inhibiting effect as 2 wt% KI. This suggests that the minimum concentration of KI needed to obtain the same oxidative inhibition effect lies in between 0.2 and 0.5 wt% KI.

4.4 LC-MS

The pre-degraded MEA samples from pilot plant A and B were sent for LC-MS analysis at an external laboratory for further assessment of degradation compounds present in the start solution, and the accumulation or formation of these compounds present in the solutions after three weeks of further experiments. The results presented in this subchapter are discussed with reports by different authors who have compared degradation compounds found in pilot scale with laboratory scale experiments.

Figure 4.6 presents the amount of MEA present in the pre-degraded MEA solutions from pilot plant A and B for day 0 and day 21. It is observed that unsalted pilot A has the greatest loss of MEA after three weeks compared to unsalted pilot B. However, it also has the highest uncertainty in the end sample. There is not observed any loss of MEA for the solution containing 2 wt% KI. Unfortunately, it was not performed a LC-MS analysis on the pilot A sample with KI due to that this experiment was still running when the samples were sent to the external laboratory for the analysis. However, it can be assumed that the solution will follow the same pattern as pilot B with KI.

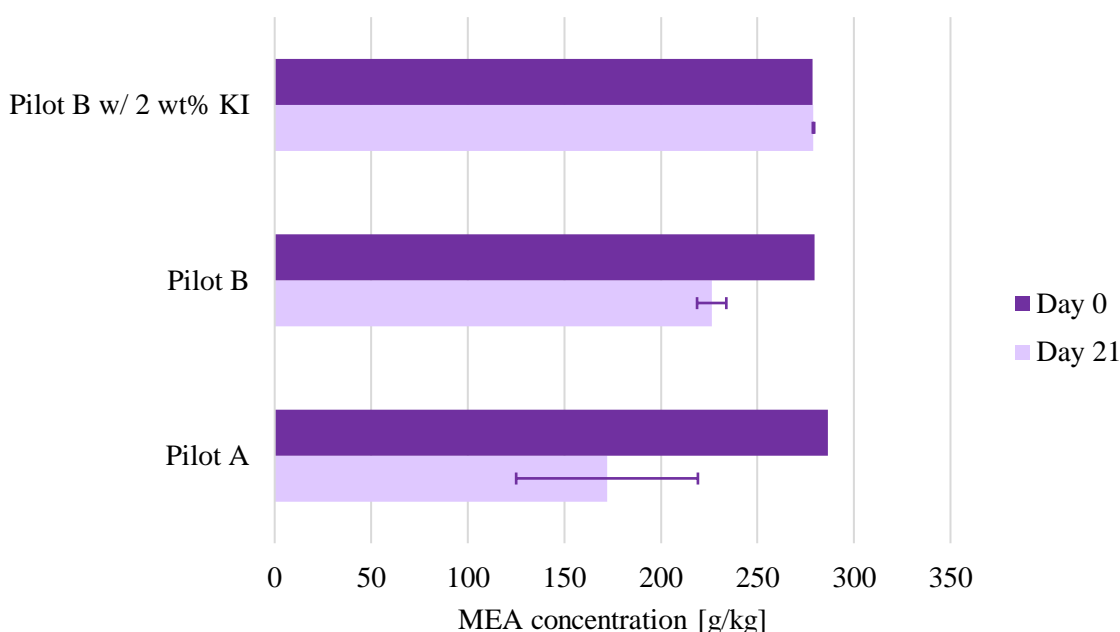


Figure 4.6. MEA concentration [g/kg] obtained from the LC-MS analysis for the unsalted pre-degraded MEA samples from pilot plant A and B and the salted pilot B solution, for day 0 and 21. All the pilot samples contain 30 wt% MEA in the initial solution. The results are corrected for water loss and loading, and the initial solutions are also corrected for pure samples. The error bars represent the standard deviation of the three parallels in each experiment. The figure is obtained from table B.10 in appendix B.

In figure 4.7-4.9 the concentration of degradation compounds in the initial- and end solution of the pre-degraded pilot samples from pilot A and B and pilot B with 2 wt% KI are presented. It is observed that the solution from pilot A contains the highest amount of HEI and HEF after 21 days compared to pilot B both with and without salt addition. Additionally, pilot A contains less degradation compounds in the initial solution compared to the other two experiments. However, it does produce the most degradation compounds after three weeks compared to pilot B with and without KI. Unsalted pilot B presents a decrease in concentration of HEPO and HeGly from day 0 to day 21. The same decrease is seen in pilot A. Unsalted pilot B has a greater increase in HEI formation after three weeks compared to pilot B with salt addition. Pilot B with 2 wt% KI contains more HeGly and

HEPO in the end solution compared to unsalted pilot B and pilot A. Generally, pilot B with salt addition has a relatively small increase in every degradation compound, compared to pilot B without salt and pilot A. It is observed a concentration of less than 1 g/kg of HEEDA, HEHEAA, HEIA, OZD and BHEOX in all the experiments compared to the other degradation compounds.

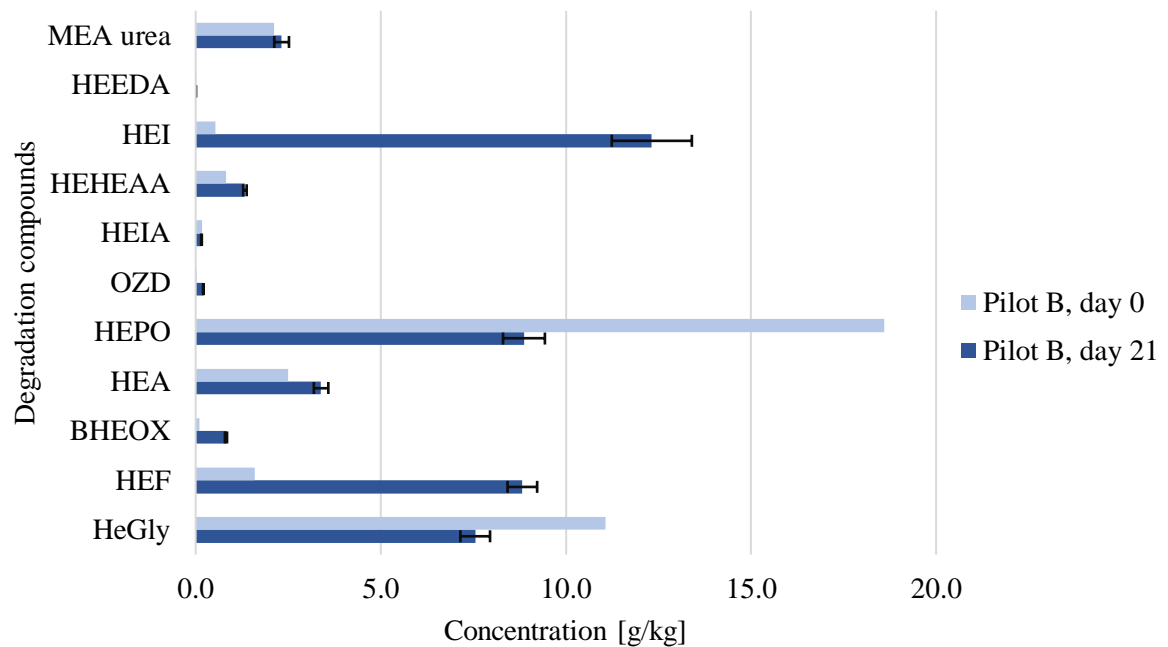


Figure 4.7. Concentration [g/kg] of degradation compounds detected in the LC-MS for the pre-degraded MEA sample from pilot plant B for day 0 and 21. The sample contain 30 wt% MEA in the initial solution. The results are corrected for water loss and loading, and the initial solutions are also corrected for pure samples. The error bars represent the standard deviation of the three parallels in each experiment. The figure is obtained from table B.10 in appendix B.

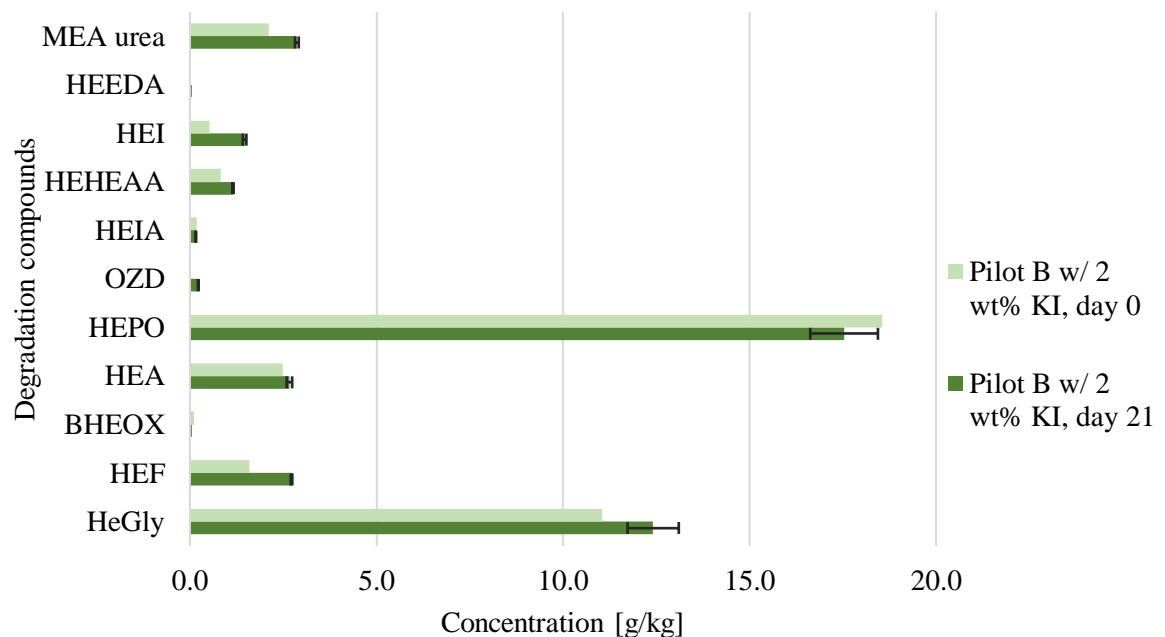


Figure 4.8. Concentration [g/kg] of degradation compounds detected in the LC-MS for the pre-degraded MEA sample from pilot plant B with 2 wt% KI for day 0 and 21. The sample contain 30 wt% MEA in the initial solution. The results are corrected for water loss and loading, and the initial solutions are also corrected for pure samples. The error bars represent the standard deviation of the three parallels in each experiment. The figure is obtained from table B.10 in appendix B.

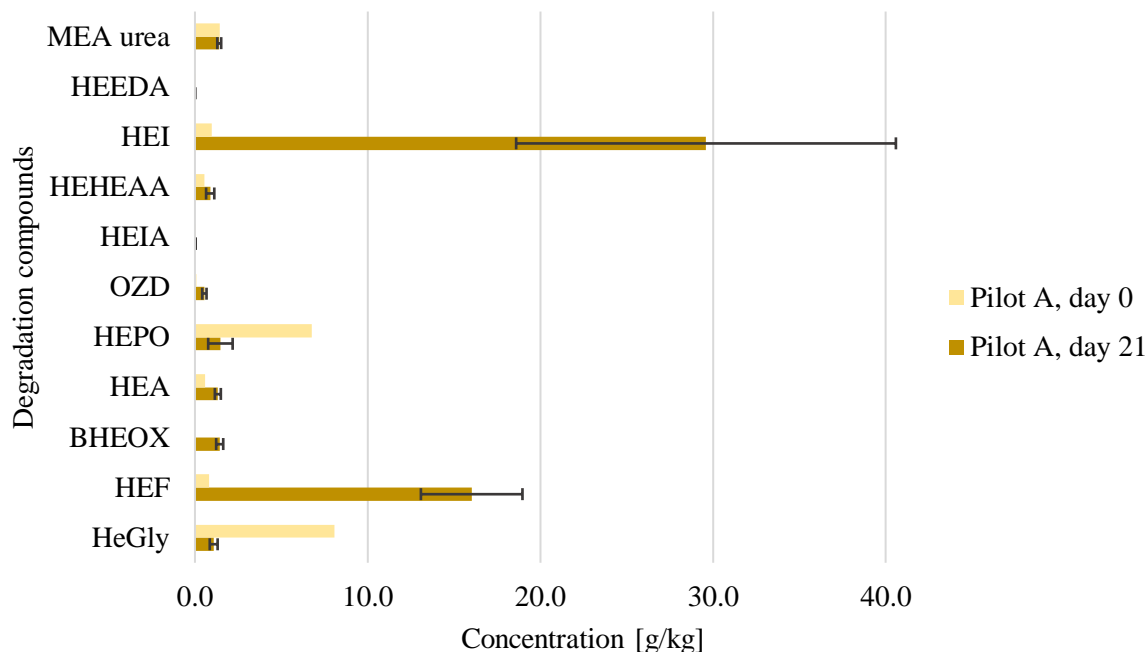


Figure 4.9. Concentration [g/kg] of degradation compounds detected in the LC-MS for the pre-degraded MEA sample from pilot plant A for day 0 and 21. The sample contain 30 wt% MEA in the initial solution. The results are corrected for water loss and loading, and the initial solutions are also corrected for pure samples. The error bars represent the standard deviation of the three parallels in each experiment. The figure is obtained from table B.10 in appendix B.

From the results presented by the LC-MS analysis it is shown that the concentrations of major- and other significant different degradation compounds vary from pilot to pilot. This is in accordance with the results presented by da Silva et al¹¹, who also observed the same effect in their study. They suggested that the solvent is exposed to more varied conditions in pilot plants than in laboratory scale, as the solvent is continuously circulated and reused it shifts between being exposed to higher temperature, oxygen levels, construction material and flue gas components, resulting in the formation of various degradation compounds. Whereas in laboratory experiments the solvent is only subjected to one set of constant conditions.

The major degradation compounds detected in the initial solutions were HEPO and HeGly, both in pilot A and B. This is in accordance with the findings of da Silva et al¹¹, who also detected HEPO and HeGly as major degradation compounds, followed by HEA and HEI as other significant degradation products. Also, Lepaumier et al³² and Strazisar et al⁴⁶ reported HEPO as a major oxidative degradation compound in pilot plants. However, Lepaumier et al³² also reported HEHEAA as one of the major degradation compounds, which is not observed in this thesis as HEHEAA is only observed in small amounts compared to other degradation compounds in the initial solutions. This result suggests that HEHEAA is an intermediate in other reactions like for example in the formation of HEPO, as suggested by da Silva et al¹¹ and Strazisar et al⁴⁶. The large concentration of HeGly and HEPO compared to the other degradation compounds in the initial solutions might be related to their formation mechanism. The reaction mechanisms are still unknown, but da Silva et al¹¹ proposed that HeGly is formed in a reaction between MEA and primary degradation compounds, while HEPO is formed in a reaction between MEA and HeGly. This could explain why it is observed more HEPO than HeGly in pilot B, as HeGly is used to produce HEPO. However, it is observed more HeGly than HEPO in pilot A, suggesting that other reactions are taking place. Another reason might be the different operating conditions in the

stripper, resulting in the different concentrations of HeGly and HEPO, as suggested by da Silva et al¹¹.

The small concentrations of OZD, HEIA and BHEOX detected in the analysis for the initial- and end solutions are in accordance with Lepaumier et al³², who also detected traces of these substance. This suggest that these compounds are intermediates in other degradation reactions, thus reacts further to produce other more stable compounds. This is supported by da Silva et al¹¹ for OZD, as they suggested it to be transient in nature, since they did not observe build up to higher concentrations of this compound in pilot plants. They also suggested that some components may be limited by chemical equilibrium. The low concentration of OZD, HEEDA and HEIA might be due to that HEEDA and HEIA are formed from OZD³², and as OZD already has a low concentration it will not produce high amounts of these degradation compounds. Another reason could be that HEEDA, HEIA and OZD are considered to be thermal degradation compounds¹¹, suggesting that they require higher temperatures than the temperature used in this work to be formed. Thus, only traces are detected in this work. Henceforth, supports the propositions that oxidative degradation dominates in pilot plants by da Silva et al¹¹, Lepaumier et al³² and Strazisar et al⁴⁶. The small concentration of BHEOX might be due to that it decomposes under stripper conditions, as suggested by Vevelstad et al⁵³, who also detected low concentration of this compound.

After three weeks under oxidative conditions, there was observed that HEF and HEI were the major degradation products formed in pilot A and unsalted pilot B. HEF and HEI were detected as the major oxidative degradation compounds in laboratory experiments and as other significant degradation compounds in pilot samples by both Lepaumier et al³² and da Silva et al¹¹. The significant increase in formation of HEI and HEF after three weeks might be due to how they are formed. HEI is believed to be formed from reactions between MEA and ammonia and various aldehydes, however the formation mechanism is still unknown^{23, 53}. Vevelstad et al⁵³ observed that HEI formation increases with increasing O₂ concentration, thereby suggesting that highly oxidative conditions increase the formation rate of HEI. This might explain the large formation of HEI as the solutions are exposed to harsh oxidative conditions (98% O₂) in this work, compared to the oxidative conditions in pilot plants. Lepaumier et al³² suggested that HEF is formed by reactions between MEA and HSS, and that this reaction strongly influence the degradation observed in pilot plants, as presented in figure 4.7 and 4.9. Also, the factors influencing the formation of HEI and HEF are still not fully understood⁵¹. The large formation of degradation compounds in pilot A compared to pilot B might be due to it having the greatest decrease in MEA concentration after three weeks, as presented in figure 4.6, and the greatest increase in HSS, as presented in figure 4.2 in section 4.1, resulting in a large formation of degradation compounds.

The noticeable amount of HEA in both the initial- and end solution in pilot B might be due to how it is formed. It is suggested to be formed in a reaction between MEA and acetic acid whereas HEF is formed from formic acid^{53, 32}. This mechanism suggests that after three weeks of further laboratory experiments under oxidative conditions more formic- than acetic acid is formed, as more HEF is produced in both pilot samples. This is in accordance with the results presented in Lepaumier et al³² and da Silva et al¹¹, where HEF was one of the major degradation compounds detected in laboratory scale. Again, the amounts of HEA detected in pilot A and B differ, as only traces of the compound are detected in pilot A in both the initial- and end solution. This suggests strongly that operating conditions vary from

pilot to pilot, as HEA was detected as a significant degradation compound by da Silva et al¹¹ but Lepaumier et al³² only detected it in trace amounts in pilot samples.

The decrease in HEPO and HeGly after three weeks in pilot A and unsalted pilot B is somewhat strange. It appears as these degradation compounds degrade further under oxidative conditions, giving rise to the interpretation that HEPO and HeGly are intermediates in other reactions, as suggested in Vevelstad et al⁵³. It is therefore suggested that both compounds contribute to the formation of HEI and HEF, resulting in the considerable increase in both HEI and HEF in pilot A and B. However, this reaction mechanism is not known. Da Silva et al¹¹ and Vevelstad et al⁵³ suggested that HEPO and HeGly require relatively high temperatures to be formed, as they observed little formation of HEPO and HeGly in their experiments under oxidative conditions. In addition, Vevelstad observed a substantial increase in HeGly formation by increasing the temperature from 55°C to 75°C. This can explain the decrease as the experiments in this thesis was run at 60°C. In both studies the concentrations of HEPO and HeGly obtained in laboratory experiments were low compared to pilot samples. The same can be said for the further experiments of the pilot samples in this thesis due to the decrease in concentration of HEPO and HeGly. This indicates that the oxidative setup is not able to capture HEPO and HeGly's behavior in pilot plants where both substances are major degradation compounds, as suggested by Vevelstad et al⁵³. Furthermore, this suggests that the oxidative setup in this thesis may not be directly translatable to the conditions in pilot facilities, as it may be suggested that the degradation reactions that are most likely to occur in pilot plants must differ from the reactions in laboratory scale. However, the continuous gas supply of 98% O₂ and continuous agitation caused by magnetic stirring provides an extremely tough oxidative environment, where compounds that are sensitive to oxidation will degrade. This alone may provide useful information regarding the stability of amines and formation of sensitive oxidative degradation compounds.

In pilot B with 2 wt% KI there is observed a very small increase in formation of every degradation compound, except for HEPO, compared to the two other experiments. This is consistent with the result presented in figure 4.6, showing no loss of MEA after three weeks. Hence, the degradation in the solution is minimal. The small decrease in HEPO and increase in HEI and HEF might be due to the low operating temperature, as explained in the section above. It is clear that addition of KI reduces formation of degradation compounds when comparing the results with unsalted pilot B, thus amine is conserved, as presented in Buvik et al⁹. However, the mechanism for how KI inhibits the degradation reactions are still not known.

In summary, the results presented in this subchapter clearly shows that the addition of KI reduces the formation of degradation compounds in pilot B under oxidative conditions, by preserving the initial MEA concentration. Thus, supporting the results presented in section 4.1 that degradation compounds already present in pilot solutions do not defeat the inhibiting effect of KI. Moreover, the major degradation compounds detected in the initial pilot solutions taken directly from the plants were HEPO and HeGly, and after three weeks of further experiments under oxidative conditions the major degradation compounds detected were HEI and HEF. These results are in accordance with da Silva et al¹¹. The decrease in HeGly and HEPO concentrations after three weeks are most likely due to the operating temperature in this work, as these compounds requires relatively high temperatures to be formed⁵³. This indicates that the oxidative setup is not able to capture HEPO and HeGly's behavior in pilot plants where both substances are major degradation

compounds. Lastly, it is shown that the concentrations of major- and other significant different degradation compounds vary from pilot to pilot, most likely due to varying operating conditions in each plant¹¹.

4.5 Viscosity

To assess if the viscosity would change significantly by the addition of KI the viscosity of the pre-degraded sample from pilot B both with and without the addition of KI were measured. This is an important parameter to assess as lower viscosities are favorable for CO₂ absorption, since it gives higher diffusivity thereby affecting the mass transfer significantly⁵⁶. In this subchapter the results from the viscosity measurements are compared to literature data given in an earlier study by Amundsen et al², on viscosity of aqueous 30 wt% MEA measured at 25°C at loadings of 0.4 and 0.5 mol CO₂/mol MEA.

Figure 4.10 presents the change in viscosity from day 0 to 21 for the pre-degraded MEA sample from pilot B both with and without the addition of KI. The addition of KI resulted in a small increase of 0.2 ± 0.3 mPa*s in viscosity compared to a decrease of 0.5 ± 0.07 mPa*s in viscosity for the unsalted solution after three weeks. For the initial solutions in both experiments the viscosity is observed to be very close. The change in viscosity versus CO₂ loading for the pre-degraded samples compared to unsalted and salted 30 wt% MEA is presented in figure 4.11. The 30 wt% MEA solutions are freshly made and have not been degraded. It is observed that the pre-degraded samples have a higher viscosity in the initial and end solution compared to 30 wt% MEA with and without KI, which appear to have similar viscosities.

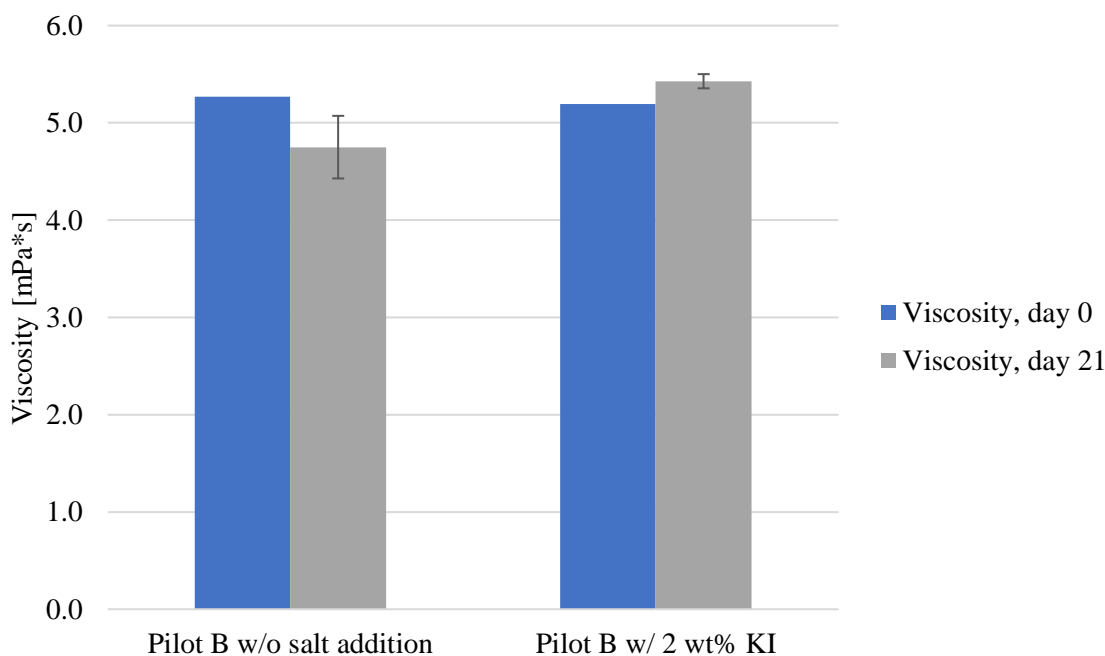


Figure 4.10. Change in viscosity from day 0 to 21 for the pre-degraded MEA samples from pilot B with and without KI. The measurements were conducted at 25°C. The error bars represent the standard deviation of the three parallels in each experiment. The figure is obtained from table B.14 in appendix B.

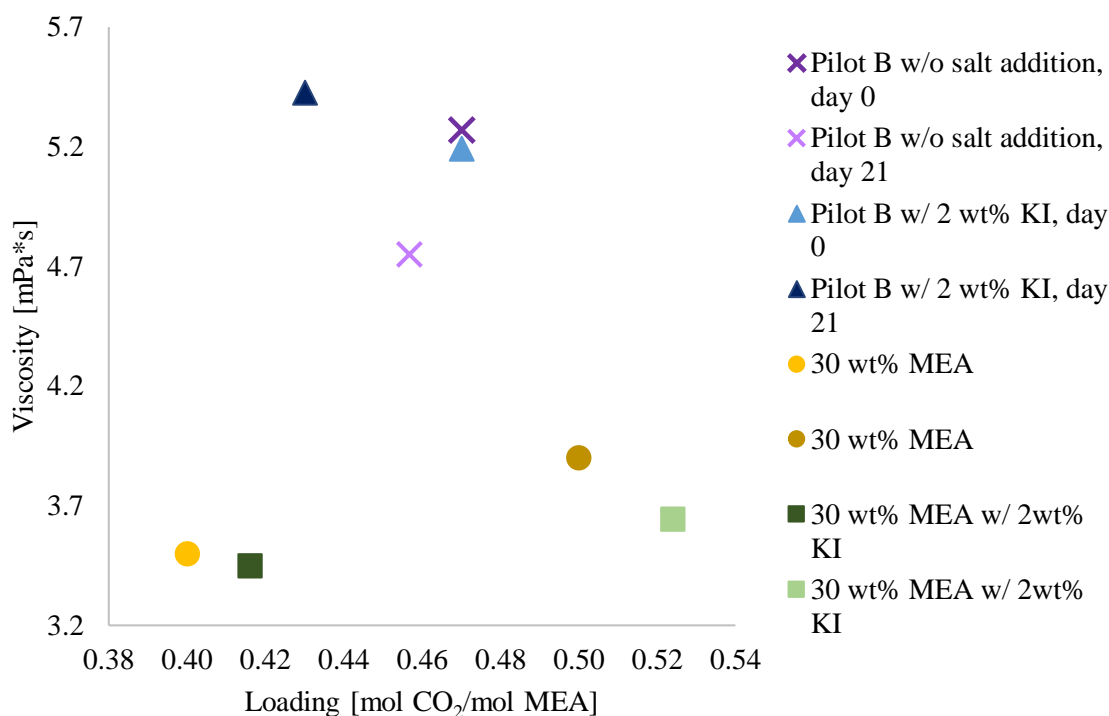


Figure 4.11. The change in viscosity versus CO₂ loading for the pre-degraded pilot samples from pilot B with and without KI, compared to unsalted 30wt% MEA and 30wt% MEA with 2wt% KI obtained from Amundsen et al² and Buvik et al⁹, respectively. All experiments were conducted at 25°C. The figure is obtained from table B.14 in appendix B.

The addition of KI in the initial pre-degraded pilot solution does not appear to influence the viscosity, as the initial viscosity in both experiments are similar and so is the loading. This is in accordance with the result presented in Buvik et al⁹, where 30 wt% MEA with 2wt% KI showed similar viscosity to a fresh 30wt% MEA solution at loadings of 0.4 and 0.5 mol CO₂/mol MEA. Buvik et al⁹ suggested that the products of the reaction between MEA and CO₂ might give a solute-solute interaction with inorganic salts, which gives the same viscosity for 30wt% MEA with and without KI at loading of 0.4 and 0.5 mol CO₂/mol MEA.

Compared to 30 wt% MEA, the pilot solutions with and without KI have a higher viscosity in the beginning and in the end of the experiments. This can be due to degradation compounds, dissolved metals and ionic degradation compounds already present in the pilot solutions. The pilot samples contain dissolved metals, which are ionic species, whereas the fresh 30 wt% MEA solutions do not. These ionic species can increase the ionic strength in the solvent, thus increasing the viscosity, as suggested by Esteves et al¹⁴ who proposed that higher ionic strength might contribute to higher viscosities. However, this is somewhat strange as KI contains ionic species and it does not appear to influence the viscosity. This might be due to that water can reduce the viscosity of ionic species⁵⁷, and since only 2 wt% KI is used in the experiments in this thesis it might not result in a significant change in viscosity. However, the significant increase in viscosity for the pre-degraded pilot solutions compared to fresh 30 wt% MEA could reduce the mass transfer in a CO₂ capture process.

The decrease in viscosity in the unsalted pilot solution after three weeks of experiment under oxidative conditions, might be due to the reduction in MEA, as presented in figure 4.6 in section 4.4, and the small decrease in loading. This naturally results in less formation of ionic products of MEA and CO₂, such as MEACOO⁻ and MEAH⁺, yielding a lower viscosity. The small increase in viscosity for the salted pre-degraded solution after three weeks, can be a result of how KI inhibit the degradation reactions, resulting in almost no

loss of MEA, as presented in figure 4.6 in section 4.4. Furthermore, after three weeks approximately 7% water has evaporated from the initial salted pilot solution. These two factors might increase the viscosity, due to 30 wt% MEA having a higher viscosity than water at 25°C, as the viscosity of water at this temperature is 0.89 mPa*s¹⁹. However, the increase in viscosity for the salted solution is almost neglectable, as it has only increased by 0.2 mPa*s after three weeks.

The salted pre-degraded pilot solution appears to show a different trend in viscosity than the one presented by both salted and unsalted fresh 30 wt% MEA, where increased loading increases the viscosity. This is might due that a reduction in loading from day 0 to 21 in the salted pilot solution gave an increase in viscosity, as mentioned earlier this might be due to the water loss and inhibition effect of KI.

In summary, the pre-degraded pilot solution showed a higher viscosity in both the initial- and end solution compared to fresh 30 wt% MEA with and without KI, which might impact the mass transfer in a CO₂ capture process. However, the addition of KI does not appear to influence the viscosity.

5. Conclusion

In this work an experimental study has been conducted on the oxidative inhibition effect of potassium iodide (KI) in pre-degraded monoethanolamine (MEA) samples from two different CO₂ capture pilot plants, the primary amines 3-amino-1-propanol (AP) and 2-(2-Aminoethoxy)ethanol (DGA) and 0.5 wt% KI in 30 wt% MEA (*aq.*) was tested to see if inhibition was still achievable.

The results presented that the addition of 2 wt% KI reduces the oxidative degradation significantly in both pilot solutions, by reducing the amine loss, formation of heat stable salts (HSS) and nitrogen containing degradation compounds after three weeks. Furthermore, it was presented that the addition of KI reduced the formation of 11 known degradation compounds, by preserving the initial MEA concentration. Thus, suggesting that the inhibition effect of KI is independent of MEA degradation compounds present in the solvent. The primary amines, DGA and AP, showed a higher oxidative stability than MEA with the addition of 2 wt% KI after three weeks, suggesting that the inhibition effect of KI is independent for primary amines. It was shown that the addition of only 0.5 wt% KI in 30 wt% MEA presented the same inhibiting effect as 2 wt% KI, suggesting that the minimum concentration of KI needed to obtain the same inhibition effect lies in between 0.2 and 0.5 wt% KI. It was observed that the addition of KI did not influence the viscosity of the initial pilot solution. Although, there was observed an increase in viscosity for the pre-degraded pilot solutions compared to fresh 30 wt% MEA, which might affect the mass transfer in a CO₂ capture process.

HEPO and HeGly were detected as the major degradation compounds in the unsalted pilot solutions taken directly from the plants, and after three weeks of further experiments under oxidative conditions the major degradation compounds detected were HEI and HEF. It was observed that the oxidative setup was not able to capture HEPO and HeGly's behavior in pilot plants, as the concentration of these compounds were reduced after three weeks of further oxidative experiments. This was suggested to be due to that HEPO and HeGly requires relatively higher temperatures than the one used in this work to be formed. Lastly, it was shown that the concentrations of major- and other significant different degradation compounds vary from pilot to pilot, most likely due to varying operating conditions in each plant.

The mechanism for which KI inhibits the oxidative degradation is still unclear but judging from the results presented in this work two mechanisms are hypothesized to be possible for the inhibition reaction of KI. The first mechanism is based on that it was observed a stable amine loss during the 21 days in all the experiments, suggesting that iodide is not consumed while inhibiting the oxidative degradation reactions. Thus, suggesting that iodide is oxidized to iodine by contact with oxidizing species then reduced back into iodide by a reducing agent. However, longer oxidative experiments than three weeks should be executed to see if the salt will be consumed due to the oxidation of the solvent. The second mechanism is based on the observation of a red precipitate accumulated on the reactor walls and the typical orange/yellow color of iron-containing solutions were not as distinct as it would have been without the addition of KI. This might suggest that KI salts out the metal from the solution, resulting in a more stable solvent under oxidative conditions. From the results presented in this thesis KI seems to be a promising oxidative degradation inhibitor for post-combustion CO₂ capture. However, further studies in pilots and cyclic systems are required to assess its applicability.

6. Suggestions for future work

There is still more work needed to be done in order to improve the understanding of the oxidative inhibition effect presented by potassium iodide (KI).

It would be interesting to run experiments over a longer period of time than three weeks with a KI concentration of 0.5 wt%, to see whether the inhibition effect will decrease after that time. Thus, presenting if KI is consumed in the reaction or not. Also, testing various KI concentrations between 0.5 and 0.2 wt% to find the minimal concentration needed to make inhibition occur would be interesting. This would be interesting from a process level point of view as operating costs could be saved. Another interesting aspect to look at from the process level is that KI can be assumed to be removed along with heat stable salts in the reclaimer, which would increase the operating expenses. However, as oxidative degradation is significantly reduced by KI the need for reclaiming would also decrease. Nevertheless, as the salt is relatively costly methods for recovering it from the reclaimer should be evaluated. Therefore, as it already exists methods for recovering iodide it should be performed feasibility studies to evaluate how easy it would be to implement these methods.

Previous studies have shown that oxidative inhibitors lose their properties when tested in cyclic systems. In this work the solvents were only exposed to harsh oxidative conditions, which are harsher than the oxidative conditions provided in pilot facilities. However, as observed from the LC-MS analysis the experimental setup was not able to capture the behavior of HEPO and HeGly in pilot plants, most likely as a result of that degradation reactions taking place in pilot plants differ from the ones taking place in lab-scale. Therefore, it is essential to test KI in cyclic systems and pilots to see how the inhibitor responds to more realistic CO₂ capture conditions, and if its inhibition effect is still functional. This will be an important step toward commercialization of KI as an inhibitor for CO₂ capture systems.

Testing KI with more amine structures are also of interest, particularly secondary and tertiary, to see if inhibition is still possible, or if longer chains and sterically hindered amines defeat this inhibition effect. As the reason behind the reduction in oxidative degradation is not yet fully understood, mechanistical studies regarding the inhibition reaction of KI would provide more insight and understanding into this phenomenon. It might also give insight regarding why it has been shown that KI is not consumed during the reaction.

Testing the viscosity of degraded pilot solutions from various pilot plants both with and without KI would also be helpful to see if the viscosity changed significantly from pilot to pilot and assess if the addition of KI would affect the mass transfer significantly. It would also be of interest to test the viscosity of various aqueous solutions of KI to see if its ionic strength will increase the viscosity, as it was not observed that the addition of KI increased the viscosity in this work. Therefore, it would be interesting to further investigate this solute-solute interaction between the products of the MEA and CO₂ reaction and the KI electrolytes.

7. References

1. Alejandro, J.; Rivera, J.; Mora-Delgado, M.-A.; Garza, V., Force Field of Monoethanolamine. *The Journal of Physical Chemistry B* **2000**, *104*, 1332.
2. Amundsen, T. G.; Øi, L. E.; Eimer, D. A., Density and Viscosity of Monoethanolamine + Water + Carbon Dioxide from (25 to 80) °C. *Journal of Chemical & Engineering Data* **2009**, *54* (11), 3096-3100.
3. Anthony J. Arduengo, I., Frederick P. Gentry, Jr. Prakash K. Taverkere, Howard E. Simmons, III Process for manufacture of imidazoles 2001.
4. Anwar, M. N.; Fayyaz, A.; Sohail, N. F.; Khokhar, M. F.; Baqar, M.; Khan, W. D.; Rasool, K.; Rehan, M.; Nizami, A. S., CO₂ capture and storage: A way forward for sustainable environment. *Journal of Environmental Management* **2018**, *226*, 131-144.
5. Bedell, S. A., Amine autoxidation in flue gas CO₂ capture—Mechanistic lessons learned from other gas treating processes. *International Journal of Greenhouse Gas Control* **2011**, *5* (1), 1-6.
6. Button, J. K.; Gubbins, K. E.; Tanaka, H.; Nakanishi, K., Molecular dynamics simulation of hydrogen bonding in monoethanolamine. *Fluid Phase Equilibria* **1996**, *116*, 320–325.
7. Buvik, V.; Bernhardsen, I. M.; Figueiredo, R. V.; Vevelstad, S. J.; Goetheer, E.; van Os, P.; Knuutila, H. K., Measurement and prediction of oxygen solubility in post-combustion CO₂ capture solvents. *International Journal of Greenhouse Gas Control* **2021**, *104*, 103205.
8. Buvik, V.; Vevelstad, S. J.; Brakstad, O. G.; Knuutila, H. K., Stability of Structurally Varied Aqueous Amines for CO₂ Capture. *Industrial & Engineering Chemistry Research* **2021**.
9. Buvik, V.; Wanderley, R. R.; Knuutila, H. K., Addition of potassium iodide reduces oxidative degradation of monoethanolamine (MEA). *Chemical Engineering Science: X* **2021**, *10*, 100096.
10. Chi, S.; Rochelle, G. T., Oxidative Degradation of Monoethanolamine. *Industrial & Engineering Chemistry Research* **2002**, *41* (17), 4178-4186.
11. da Silva, E. F.; Lepaumier, H.; Grimstvedt, A.; Vevelstad, S. J.; Einbu, A.; Vernstad, K.; Svendsen, H. F.; Zahlsen, K., Understanding 2-Ethanolamine Degradation in Postcombustion CO₂ Capture. *Industrial & Engineering Chemistry Research* **2012**, *51* (41), 13329-13338.
12. Dennis, W.; Hull, L.; Rosenblatt, D., Oxidations of amines. IV. Oxidative fragmentation. *The Journal of Organic Chemistry* **1967**, *32*.
13. Dhingra, S.; Khakharia, P.; Rieder, A.; Cousins, A.; Reynolds, A.; Knudsen, J.; Andersen, J.; Irons, R.; Mertens, J.; Abu Zahra, M.; Os, P.; Goetheer, E., Understanding and Modelling the Effect of Dissolved Metals on Solvent Degradation

- in Post Combustion CO₂ Capture Based on Pilot Plant Experience. *Energies* **2017**, *10*, 629.
14. Esteves, M. J. C.; Cardoso, M. J. E. d. M.; Barcia, O. E., A Debye–Hückel Model for Calculating the Viscosity of Binary Strong Electrolyte Solutions. *Industrial & Engineering Chemistry Research* **2001**, *40* (22), 5021-5028.
 15. Feron, P. H. M., 1 - Introduction. In *Absorption-Based Post-combustion Capture of Carbon Dioxide*, Feron, P. H. M., Ed. Woodhead Publishing: 2016; pp 3-12.
 16. Feron, P. H. M.; Cousins, A.; Jiang, K.; Zhai, R.; Garcia, M., An update of the benchmark post-combustion CO₂-capture technology. *Fuel* **2020**, *273*, 117776.
 17. Fredriksen, S. B.; Jens, K.-J., Oxidative Degradation of Aqueous Amine Solutions of MEA, AMP, MDEA, Pz: A Review. *Energy Procedia* **2013**, *37*, 1770-1777.
 18. Fytianos, G.; Vevelstad, S. J.; Knuutila, H. K., Degradation and corrosion inhibitors for MEA-based CO₂ capture plants. *International Journal of Greenhouse Gas Control* **2016**, *50*, 240-247.
 19. GmbH, A. P. Viscosity of Water. <https://wiki.anton-paar.com/en/water/> (accessed 22.06.21).
 20. Goff, G. S. Oxidative Degradation of Aqueous Monoethanolamine in CO₂ Capture Processes: Iron and Copper Catalysis, Inhibition, and O₂ Mass Transfer Dissertation, The University of Texas at Austin, 2005.
 21. Goff, G. S.; Rochelle, G. T., Monoethanolamine Degradation: O₂ Mass Transfer Effects under CO₂ Capture Conditions. *Industrial & Engineering Chemistry Research* **2004**, *43* (20), 6400-6408.
 22. Goff, G. S.; Rochelle, G. T., Oxidation Inhibitors for Copper and Iron Catalyzed Degradation of Monoethanolamine in CO₂ Capture Processes. *Industrial & Engineering Chemistry Research* **2006**, *45* (8), 2513-2521.
 23. Gouedard, C.; Picq, D.; Launay, F.; Carrette, P. L., Amine degradation in CO₂ capture. I. A review. *International Journal of Greenhouse Gas Control* **2012**, *10*, 244-270.
 24. Grace, J., Understanding and managing the global carbon cycle. *Journal of Ecology* **2004**, *92*, 189-202.
 25. Hoegh-Guldberg, O., D. Jacob, M. Taylor, M. Bindi, S. Brown, I. Camilloni, A. Diedhiou, R. Djalante, K.L. Ebi, F. Engelbrecht, J. Guiot, Y. Hijioka, S. Mehrotra, A. Payne, S.I. Seneviratne, A. Thomas, R. Warren, and G. Zhou, *Impacts of 1.5°C Global Warming on Natural and Human Systems.*; Intergovernmental Panel on Climate Change: <https://www.ipcc.ch/>, 2018.
 26. Hull, L.; Davis, G.; Rosenblatt, D.; Williams, H.; Weglein, R., Oxidations of Amines. III. Duality of Mechanism in the Reaction of Amines with Chlorine Dioxide. *Journal of the American Chemical Society* **1967**, *89*.

27. IEA Global CO₂ emissions in 2019. <https://www.iea.org/articles/global-co2-emissions-in-2019>.
28. IPCC *Climate Change 2014: Synthesis Report. Contribution of Working Groups I, II and III to the Fifth Assessment Report of the Intergovernmental Panel on Climate Change [Core Writing Team, R.K. Pachauri and L.A. Meyer (eds.)]*; IPCC: Geneva, Switzerland, 2014; p 151.
29. Keeling, C. D., & Whorf, T. P., Monthly Atmospheric CO₂ Records from Sites in the SIO Air Sampling Network. United States. States), E. S. S. D. I. f. a. V. E. E.-D. U., Ed. 2004.
30. Lee, Y. J.; Rochelle, G. T., Oxidative degradation of organic acid conjugated with sulfite oxidation in flue gas desulfurization: products, kinetics, and mechanism. *Environmental Science & Technology* **1987**, *21* (3), 266-272.
31. Léonard, G.; Voice, A.; Toye, D.; Heyen, G., Influence of Dissolved Metals and Oxidative Degradation Inhibitors on the Oxidative and Thermal Degradation of Monoethanolamine in Postcombustion CO₂ Capture. *Industrial & Engineering Chemistry Research* **2014**, *53* (47), 18121-18129.
32. Lepaumier, H.; da Silva, E. F.; Einbu, A.; Grimstvedt, A.; Knudsen, J. N.; Zahlse, K.; Svendsen, H. F., Comparison of MEA degradation in pilot-scale with lab-scale experiments. *Energy Procedia* **2011**, *4*, 1652-1659.
33. Lepaumier, H.; Picq, D.; Carrette, P.-L., New Amines for CO₂ Capture. I. Mechanisms of Amine Degradation in the Presence of CO₂. *Industrial & Engineering Chemistry Research* **2009**, *48* (20), 9061-9067.
34. Lepaumier, H.; Picq, D.; Carrette, P.-L., New Amines for CO₂ Capture. II. Oxidative Degradation Mechanisms. *Industrial & Engineering Chemistry Research* **2009**, *48* (20), 9068-9075.
35. Ma'mun, S.; Jakobsen, J. P.; Svendsen, H. F.; Juliussen, O., Experimental and Modeling Study of the Solubility of Carbon Dioxide in Aqueous 30 Mass % 2-((2-Aminoethyl)amino)ethanol Solution. *Industrial & Engineering Chemistry Research* **2006**, *45* (8), 2505-2512.
36. Petryaev, E. P.; Pavlov, A. V.; Shadyro, O. I., Homolytic deamination of amino alcohols. *Journal of Organic Chemistry of the USSR* **1984**, *20*, 25-29.
37. Puxty, G.; Maeder, M., 2 - The fundamentals of post-combustion capture. In *Absorption-Based Post-combustion Capture of Carbon Dioxide*, Feron, P. H. M., Ed. Woodhead Publishing: 2016; pp 13-33.
38. Reynolds, A. J.; Verheyen, T. V.; Adeloju, S. B.; Chaffee, A. L.; Meuleman, E., Evaluation of methods for monitoring MEA degradation during pilot scale post-combustion capture of CO₂. *International Journal of Greenhouse Gas Control* **2015**, *39*, 407-419.

39. Reynolds, A. J.; Verheyen, T. V.; Meuleman, E., 16 - Degradation of amine-based solvents. In *Absorption-Based Post-combustion Capture of Carbon Dioxide*, Feron, P. H. M., Ed. Woodhead Publishing: 2016; pp 399-423.
40. Rosenblatt, D.; Hayes, A.; Harrison, B.; Streaty, R.; Moore, K., The Reaction of Chlorine Dioxide with Triethylamine in Aqueous Solution1. *Journal of Organic Chemistry - J ORG CHEM* **1963**, *28*.
41. Rosenblatt, D.; Hull, L.; Luca, D.; Davis, G.; Weglein, R.; Williams, H., Oxidations of Amines. II. Substituent Effects in Chlorine Dioxide Oxidations. *Journal of the American Chemical Society* **1967**, *89*.
42. Ruddiman, W., How Did Humans First Alter Global Climate? *Scientific American* **2005**, *292*, 34-41.
43. Sanna, A.; Vega, F.; Navarrete, B.; Maroto-Valer, M. M., Accelerated MEA Degradation Study in Hybrid CO₂ Capture Systems. *Energy Procedia* **2014**, *63*, 745-749.
44. Sjostrom Sharon, B. E. K., Constance Senior Control of wet scrubber oxidation inhibitor and byproduct recovery. US 10,758,863 B2 2020.
45. Song, C.; Liu, Q.; Deng, S.; Li, H.; Kitamura, Y., Cryogenic-based CO₂ capture technologies: State-of-the-art developments and current challenges. *Renewable and Sustainable Energy Reviews* **2019**, *101*, 265-278.
46. Strazisar, B. R.; Anderson, R. R.; White, C. M., Degradation Pathways for Monoethanolamine in a CO₂ Capture Facility. *Energy & Fuels* **2003**, *17* (4), 1034-1039.
47. Supap, T.; Idem, R.; Tontiwachwuthikul, P., Mechanism of formation of heat stable salts (HSSs) and their roles in further degradation of monoethanolamine during CO₂ capture from flue gas streams. *Energy Procedia* **2011**, *4*, 591-598.
48. Tobiesen, F. A.; Svendsen, H. F., Study of a Modified Amine-Based Regeneration Unit. *Industrial & Engineering Chemistry Research* **2006**, *45* (8), 2489-2496.
49. Vega, F.; Sanna, A.; Navarrete, B.; Maroto-Valer, M. M.; Cortés, V. J., Degradation of amine-based solvents in CO₂ capture process by chemical absorption. *Greenhouse Gases: Science and Technology* **2014**, *4* (6), 707-733.
50. Vevelstad, S. J. CO₂ absorbent degradation. Norwegian University of Science and Technology (NTNU), 2013.
51. Vevelstad, S. J.; Grimstvedt, A.; Elnan, J.; da Silva, E. F.; Svendsen, H. F., Oxidative degradation of 2-ethanolamine: The effect of oxygen concentration and temperature on product formation. *International Journal of Greenhouse Gas Control* **2013**, *18*, 88-100.
52. Vevelstad, S. J.; Grimstvedt, A.; Knuutila, H.; da Silva, E. F.; Svendsen, H. F., Influence of experimental setup on amine degradation. *International Journal of Greenhouse Gas Control* **2014**, *28*, 156-167.

53. Vevelstad, S. J.; Johansen, M. T.; Knuutila, H.; Svendsen, H. F., Extensive dataset for oxidative degradation of ethanolamine at 55–75°C and oxygen concentrations from 6 to 98%. *International Journal of Greenhouse Gas Control* **2016**, *50*, 158-178.
54. Voice, A. K.; Rochelle, G. T., Inhibitors of Monoethanolamine Oxidation in CO₂ Capture Processes. *Industrial & Engineering Chemistry Research* **2014**, *53* (42), 16222-16228.
55. Vorobyov, I.; Yappert, M.; DuPré, D., Hydrogen Bonding in Monomers and Dimers of 2-Aminoethanol. *Journal of Physical Chemistry A - J PHYS CHEM A* **2002**, *106*.
56. Xiao, M.; Liu, H.; Gao, H.; Olson, W.; Liang, Z., CO₂ capture with hybrid absorbents of low viscosity imidazolium-based ionic liquids and amine. *Applied Energy* **2019**, *235*, 311-319.
57. Yang, J.; Yu, X.; Yan, J.; Tu, S.-T., CO₂ Capture Using Amine Solution Mixed with Ionic Liquid. *Industrial & Engineering Chemistry Research* **2014**, *53* (7), 2790-2799.

Appendix A: Material and Methods

Equation (A.1) was used to correct from a CO₂-loaded solution to an unloaded solution by using the concentration [g/kg] of CO₂ measured by the TIC analysis ($C_{CO_2 \text{ from TIC}}$) and the amine concentration [mol/kg] measured by amine titration ($C_{titration}$).

$$C_{unloaded} = \frac{C_{titration} * (C_{CO_2 \text{ from TIC}} + 1000g)}{1000 g} \quad (A.1)$$

It was assumed a linear loss of water during the experiment to correct for water and degradation losses. This is shown in equation (A.2), where $C_{unloaded}$ is the concentration [mol/kg] of amine in the unloaded solution calculated by equation (A.1), Day is the time in days for when the sample was taken, $slope$ is the value of the slope of the water loss curve and $C_{corrected}$ is the concentration [mol/kg] of amine in the solution after correction of water loss and loading.

$$C_{corrected} = C_{unloaded} - (Day * slope * C_{unloaded}) \quad (A.2)$$

The standard deviation (SD) of the parallels in each experiment were calculated according to equation (A.3), where n is the number of samples, \bar{x} is the sample average and x_i is the measured concentration of each sample.

$$SD = \sqrt{\frac{\sum_{i=1}^n (x_i - \bar{x})^2}{n - 1}} \quad (A.3)$$

Equation (A.4) was used to correct from the pure pre-degraded MEA pilot sample taken directly from the plant to the initial 30 wt% MEA pre-degrade pilot solution used in the experiments in this thesis. This equation was used on the results for the initial solutions obtained in the LC-MS analysis. $C_{original \text{ solution, LC-MS}}$ is the concentration [g/kg] of degradation compounds from the LC-MS analysis, $m_{original \text{ solution in start solution}}$ is the amount [g] of the pre-degraded MEA sample added into the initial solution and $m_{total \text{ start solution}}$ is the total mass [g] of the initial solution. To calculate the concentration of MEA in the initial pre-degraded solution used in this work the amount of pure MEA [g] added was added to equation (A.4).

$$\frac{C_{original \text{ solution, LC-MS}} * m_{original \text{ solution in start solution}}}{m_{total \text{ start solution}}} \quad (A.4)$$

Table A.1. Amount of MEA, H₂O, Glycolic acid (GA) and acetic acid (AA.) added to a 30wt% MEA solution to produce artificial HSS with known concentration.

<i>Name</i>	<i>MEA [g]</i>	<i>H₂O [g]</i>	<i>Acetic acid [g]</i>	<i>Glycolic acid [g]</i>	<i>Total [g]</i>	<i>MEA [wt%]</i>	<i>H₂O [wt%]</i>	<i>HSS [wt%]</i>	<i>conc HSS [mol/kg]</i>
<i>MEA + AA</i>	29,74	70,78	0,66		101,18	29 %	70 %	1 %	0,109
<i>MEA + GA</i>	30,04	73,05		0,8186	103,91	29 %	70 %	1 %	0,104
<i>MEA</i>	210,17	490,2			700,37	30 %	70 %	0 %	0,000

Table A.2. Amount of sample of the solution with known concentration of HSS, NaOH used to get to the first equivalence point and the measured concentration of HSS for each parallel. The calculated average concentration of HSS in each sample with the average uncertainty calculated as the difference between the measured concentration of HSS and the known concentration of HSS.

<i>Name</i>	<i>Parallell</i>	<i>Sample [g]</i>	<i>NaOH [mL]</i>	<i>HSS [mol/k)</i>	<i>Average HSS [mol/kg]</i>	<i>Average Deviation [%]</i>	<i>Average Deviation [mol/kg]</i>
<i>MEA+GA</i>	1	1,822	3,7070	0,10	3,79040	1 %	0,001
	2	1,828	3,8738	0,11			
<i>MEA+AA</i>	1	1,797	4,0532	0,11	4,14915	6 %	0,006
	2	1,811	4,2451	0,12			
<i>MEA</i>	1	1,775	0,3160	0,01			0,01
	2						

Table A.3. Raw data from the LC-MS analysis.

<i>Experiment</i>	<i>MEA</i> [g/kg]	<i>HeGly</i> [g/kg]	<i>HEF</i> [g/kg]	<i>BHEOX</i> [g/kg]	<i>HEA</i> [g/kg]	<i>HEPO</i> [g/kg]	<i>OZD</i> [g/kg]	<i>HEIA</i> [g/kg]	<i>HEHEAA</i> [g/kg]	<i>HEI</i> [g/kg]	<i>HEEDA</i> [g/kg]	<i>MEA</i> <i>urea</i> [g/kg]
<i>Pilot A start (pure)</i>	233,5	8,10	0,82	< 0,10	0,58	6,78	0,09	0,036	0,56	0,98	0,0022	1,45
<i>Pilot A end, day 21a</i>	217,1	1,25	12,97	1,61	1,10	2,19	0,39	0,026	1,10	16,72	0,0014	1,25
<i>Pilot A end, day 21b</i>	162,7	1,13	15,47	1,23	1,41	1,33	0,58	0,030	0,85	33,34	< 0,001	1,48
<i>Pilot A end, day 21c</i>	129,3	0,84	19,14	1,40	1,42	0,84	0,64	0,028	0,66	37,95	< 0,001	1,45
<i>Pilot B start (pure)</i>	218,3	11,92	1,71	0,11	2,69	20,02	0,03	0,194	0,88	0,56	0,0034	2,29
<i>Pilot B end, day 21a</i>	217,5	7,06	8,79	0,82	3,18	8,18	0,21	0,148	1,27	12,19	0,0048	2,22
<i>Pilot B end, day 21b</i>	227,7	7,73	8,48	0,79	3,39	9,12	0,20	0,156	1,39	11,35	0,0046	2,20
<i>Pilot B end, day 21c</i>	228,3	7,68	8,98	0,82	3,50	9,09	0,20	0,163	1,30	13,09	0,0045	2,49
<i>Pilot B end, day 21a, KI</i>	276,6	12,20	2,72	< 0,10	2,56	16,59	0,21	0,160	1,16	1,47	< 0,001	2,80
<i>Pilot B end, day 21b, KI</i>	275,1	12,95	2,67	< 0,10	2,66	18,22	0,23	0,156	1,14	1,48	< 0,001	2,81
<i>Pilot B end, day 21c, KI</i>	276,7	11,71	2,69	< 0,10	2,69	17,24	0,23	0,158	1,12	1,40	< 0,001	2,90

Appendix B: Results and Discussion

Table B.1. Data obtained from the oxidative degradation setup for each parallel on each sample day, for the experiment with predegraded MEA from pilot A with 2 wt% KI at 60°C. Average alkalinity was calculated as an average of the three parallels on each sample day and is corrected for water loss and loading. Amine remaining was calculated as the percentage of amine left compared to day 0 and it's given with its uncertainty, which was calculated as the standard deviation of the three parallels. The loading was calculated assuming that the alkalinity measured by titration stands for MEA in the solvent.

<i>Pilot A (30 wt% MEA) w/ 2 wt% KI</i>							
Day	Total alkalinity w/ CO₂ [mol/kg]	CO₂ conc. [g/kg]	Loading [mol CO₂/mol MEA]	Alkalinity w/o CO₂ [mol/kg]	Alkalinity corrected [mol/kg]	Avg. alkalinty corrected [mol/kg]	Amine remaining [%]
0	4,45	85,14	0,44	4,82	4,82	4,82	100 % ± 0,0%
3a	4,42	86,17	0,44	4,80	4,75		
3b	4,41	86,76	0,45	4,79	4,74	4,74	98 % ± 0,3%
3c	4,38	86,60	0,45	4,76	4,73		
7a	4,41	85,70	0,44	4,79	4,69		
7b	4,43	86,32	0,44	4,81	4,71	4,69	97 % ± 0,2%
7c	4,38	86,31	0,45	4,76	4,68		
10a	4,43	86,10	0,44	4,81	4,67		
10b	4,44	86,47	0,44	4,83	4,68	4,67	97 % ± 0,1%
10c	4,40	86,32	0,45	4,78	4,67		
14a	4,46	86,95	0,44	4,84	4,65		
14b	4,44	86,69	0,44	4,82	4,61	4,63	96 % ± 0,4%
14c	4,40	85,66	0,44	4,78	4,63		
17a	4,45	87,07	0,44	4,84	4,60		
17b	4,48	86,40	0,44	4,87	4,61	4,60	95 % ± 0,1%
17c	4,41	86,39	0,45	4,79	4,60		
21a	4,49	87,84	0,44	4,88	4,59		
21b	4,51	85,91	0,43	4,90	4,58	4,59	95 % ± 0,3%
21c	4,46	85,83	0,44	4,85	4,61		

Table B.2. Data obtained from the oxidative degradation setup for each parallel on each sample day for the experiment with predegraded MEA from pilot A without salt addition at 60°C. Average alkalinity was calculated as an average of the three parallels on each sample day and is corrected for water loss and loading. Amine remaining was calculated as the percentage of amine left compared to day 0 and it's given with its uncertainty, which was calculated as the standard deviation of the three parallels. The loading was calculated assuming that the alkalinity measured by titration stands for MEA in the solvent.

<i>Pilot A (30 wt% MEA) w/o salt addition</i>							
Day	Total alkalinity w/ CO₂ [mol/kg]	CO₂ conc. [g/kg]	Loading [mol CO₂/mol MEA]	Alkalinity w/o CO₂ [mol/kg]	Alkalinity corrected [mol/kg]	Avg. alkalinty corrected [mol/kg]	Amine remaining [%]
0	4,48	81,00	0,41	4,85	4,85	4,85	100 % ± 0,0%
3a	4,36	83,78	0,44	4,73	4,70		
3b	4,31	77,94	0,41	4,64	4,62	4,66	96% ± 0,8%
3c	4,34	79,56	0,42	4,69	4,67		
7a	4,24	83,39	0,45	4,59	4,53		
7b	4,04	76,48	0,42	4,34	4,29	4,40	91% ± 2,4%
7c	4,12	76,48	0,42	4,43	4,38		
10a	4,12	80,03	0,44	4,45	4,36		
10b	3,84	69,93	0,41	4,10	4,04	4,18	86% ± 3,4%
10c	3,91	71,12	0,41	4,19	4,12		
14a	3,94	76,85	0,44	4,24	4,12		
14b	3,48	63,31	0,41	3,70	3,62	3,75	77% ± 6,7%
14c	3,38	61,42	0,41	3,59	3,51		
17a	3,80	74,05	0,44	4,08	3,94		
17b	3,21	57,15	0,41	3,39	3,30	3,41	70% ± 10,0%
17c	2,93	49,23	0,38	3,07	2,99		
21a	3,58	69,95	0,44	3,83	3,67		
21b	2,77	44,31	0,36	2,89	2,80	2,93	61% ± 13,9%
21c	2,34	34,60	0,34	2,42	2,34		

Table B.3. Data obtained from the oxidative degradation setup for each parallel on each sample day for the experiment with predegraded MEA from pilot B with 2 wt% KI at 60°C. Average alkalinity was calculated as an average of the three parallels on each sample day and is corrected for water loss and loading. Amine remaining was calculated as the percentage of amine left compared to day 0 and it's given with its uncertainty, which was calculated as the standard deviation of the three parallels. The loading was calculated assuming that the alkalinity measured by titration stands for MEA in the solvent.

<i>Pilot B (30 wt% MEA) w/ 2 wt% KI</i>							
Day	Total alkalinity w/ CO₂ [mol/kg]	CO₂ conc. [g/kg]	Loading [mol CO₂/mol MEA]	Alkalinity w/o CO₂ [mol/kg]	Alkalinity corrected [mol/kg]	Avg. alkalinty corrected [mol/kg]	Amine remaining [%]
0	4,40	90,25	0,47	4,79	4,79	4,79	100 % ± 0,0%
3a	4,44	82,91	0,42	4,81	4,76		
3b	4,42	83,57	0,43	4,78	4,74	4,74	99% ± 0,5%
3c	4,39	83,31	0,43	4,76	4,71		
7a	4,38	82,74	0,43	4,74	4,63		
7b	4,37	84,33	0,44	4,74	4,64	4,64	97% ± 0,1%
7c	4,38	83,18	0,43	4,74	4,63		
10a	4,43	82,64	0,42	4,80	4,64		
10b	4,36	84,25	0,44	4,73	4,59	4,61	96% ± 0,5%
10c	4,39	84,17	0,44	4,76	4,60		
14a	4,40	83,48	0,43	4,76	4,54		
14b	4,35	82,55	0,43	4,71	4,51	4,53	95% ± 0,3%
14c	4,39	83,47	0,43	4,75	4,53		
17a	4,40	81,73	0,42	4,76	4,50		
17b	4,36	83,52	0,44	4,72	4,49	4,50	94% ± 0,1%
17c	4,40	83,65	0,43	4,77	4,50		
21a	4,43	82,98	0,43	4,79	4,46		
21b	4,36	81,66	0,43	4,72	4,43	4,44	93% ± 0,3%
21c	4,40	83,04	0,43	4,77	4,43		

Table B.4. Data obtained from the oxidative degradation setup for each parallel on each sample day for the experiment with predegraded MEA from pilot B without salt addition at 60°C. Average alkalinity was calculated as an average of the three parallels on each sample day and is corrected for water loss and loading. Amine remaining was calculated as the percentage of amine left compared to day 0 and it's given with its uncertainty, which was calculated as the standard deviation of the three parallels. The loading was calculated assuming that the alkalinity measured by titration stands for MEA in the solvent.

<i>Pilot B (30 wt% MEA) w/o salt addition</i>							
Day	Total alkalinity w/ CO₂ [mol/kg]	CO₂ conc. [g/kg]	Loading [mol CO₂/mol MEA]	Alkalinity w/o CO₂ [mol/kg]	Alkalinity corrected [mol/kg]	Avg. alkalinty corrected [mol/kg]	Amine remaining [%]
0	4,46	92,71	0,47	4,87	4,87	4,87	100 % ± 0,0%
3a	4,42	89,01	0,46	4,82	4,78		
3b	4,41	87,57	0,45	4,80	4,75	4,76	98% ± 0,4%
3c	4,40	87,58	0,45	4,78	4,75		
7a	4,27	88,27	0,47	4,64	4,55		
7b	4,25	86,22	0,46	4,62	4,51	4,52	93% ± 0,5%
7c	4,23	85,30	0,46	4,59	4,51		
10a	4,14	83,15	0,46	4,49	4,36		
10b	4,14	82,41	0,45	4,49	4,33	4,35	89% ± 0,4%
10c	4,12	84,04	0,46	4,46	4,36		
14a	3,95	78,30	0,45	4,26	4,10		
14b	3,97	79,28	0,45	4,28	4,07	4,09	84% ± 0,2%
14c	3,93	77,68	0,45	4,23	4,09		
17a	3,78	72,82	0,44	4,05	3,86		
17b	3,82	75,62	0,45	4,11	3,87	3,87	80% ± 0,4%
17c	3,78	75,13	0,45	4,06	3,90		
21a	3,54	69,97	0,45	4,79	3,57		
21b	3,64	70,52	0,44	3,89	3,61	3,69	76% ± 3,6%
21c	3,79	80,05	0,48	4,09	3,89		

Table B.5. Data obtained from the oxidative degradation setup for each parallel on each sample day for the experiment with 30 wt% AP⁴ with 2 wt% KI at 60°C. Average alkalinity was calculated as an average of the three parallels on each sample day and is corrected for water loss and loading. Amine remaining was calculated as the percentage of amine left compared to day 0 and it's given with its uncertainty, which was calculated as the standard deviation of the three parallels. The loading was calculated assuming that the alkalinity measured by titration stands for MEA in the solvent.

30 wt% AP (aq.) with 2 wt% KI							
Day	Total alkalinity w/ CO ₂ [mol/kg]	CO ₂ conc. [g/kg]	Loading [mol CO ₂ /mol MEA]	Alkalinity w/o CO ₂ [mol/kg]	Alkalinity corrected [mol/kg]	Avg. alkalinty corrected [mol/kg]	Amine remaining [%]
0	3,74	71,73	0,44	4,01	4,01	4,01	100 % ± 0,0%
3a	3,73	78,68	0,48	4,03	4,00		
3b	3,74	79,10	0,48	4,04	4,02	4,00	100% ± 0,5%
3c	3,71	80,01	0,49	4,00	3,98		
7a	3,75	80,03	0,49	4,05	3,99		
7b	3,76	82,41	0,50	4,07	4,02	4,00	100% ± 0,4%
7c	3,75	80,78	0,49	4,05	3,99		
10a	3,78	79,83	0,48	4,08	4,00		
10b	3,79	80,43	0,48	4,09	4,02	4,00	100% ± 0,5%
10c	3,76	80,09	0,48	4,06	3,98		
14a	3,80	78,87	0,47	4,10	3,98		
14b	3,81	81,00	0,48	4,11	4,01	3,99	100% ± 0,4%
14c	3,80	80,85	0,48	4,10	3,99		
17a	3,85	81,01	0,48	4,16	4,02		
17b	3,83	81,07	0,48	4,14	4,01	4,01	100% ± 0,2%
17c	3,82	85,34	0,51	4,15	4,00		
21a	3,86	81,15	0,48	4,18	4,00		
21b	3,88	82,56	0,48	4,20	4,04	4,03	100% ± 0,5%
21c	3,89	81,63	0,48	4,21	4,03		

Table B.6. Data obtained from the oxidative degradation setup for each parallel on each sample day for the experiment with 30 wt% DGA⁴ with 2 wt% KI at 60°C. Average alkalinity was calculated as an average of the three parallels on each sample day and is corrected for water loss and loading. Amine remaining was calculated as the percentage of amine left compared to day 0 and it's given with its uncertainty, which was calculated as the standard deviation of the three parallels. The loading was calculated assuming that the alkalinity measured by titration stands for MEA in the solvent. The CO₂ concentration was calculated from the assumed loading from Buvik et al and the titration results with CO₂ from the experiment in this thesis.

30 wt% DGA (aq.) with 2 wt% KI							
Day	Total alkalinity w/ CO ₂ [mol/kg]	CO ₂ conc. [g/kg]	Loading ¹ [mol CO ₂ /mol MEA]	Alkalinity w/o CO ₂ [mol/kg]	Alkalinity corrected [mol/kg]	Avg. alkalinty corrected [mol/kg]	Amine remaining [%]
0	2,71	53,67	0,45	2,86	2,86	2,86	100% ± 0,0%
3a	2,74	48,24	0,40	2,87	2,85		
3b	2,74	48,16	0,40	2,87	2,85	2,85	100% ± 0,1%
3c	2,74	48,25	0,40	2,87	2,85		
7a	2,75	47,22	0,39	2,88	2,83		
7b	2,75	47,15	0,39	2,88	2,83	2,83	99% ± 0,1%
7c	2,75	47,26	0,39	2,88	2,83		
10a	2,75	47,27	0,39	2,88	2,81		
10b	2,77	47,48	0,39	2,90	2,83	2,83	99% ± 0,5%
10c	2,78	47,68	0,39	2,91	2,84		
14a	2,77	47,56	0,39	2,90	2,80		
14b	2,79	47,82	0,39	2,92	2,82	2,81	99% ± 0,4%
14c	2,78	46,56	0,38	2,91	2,82		
17a	2,78	47,79	0,39	2,92	2,79		
17b	2,80	48,06	0,39	2,93	2,81	2,80	98% ± 0,6%
17c	2,77	47,53	0,39	2,90	2,78		
21a	2,83	47,30	0,38	2,96	2,81		
21b	2,82	47,10	0,38	2,95	2,80	2,80	98% ± 0,2%
21c	2,81	47,00	0,38	2,94	2,79		

¹ The assumption that the loading in the salted DGA solution is equal to the unsalted solution, as explained in section 3.2.3.2, might provide a small error in the results. However, this error should be very small, since the exact same oxidative degradation set up with the same oxidative conditions (temperature, loading, gas flow and gas compositions) was used. In addition, the exact same experimental procedures were also utilized. Hence, the only difference between the execution of the experiments is the addition of KI, which by comparing the loadings presented for 30 wt% MEA with and without KI in the supplementary information given in Buvik et al⁹, might give an indication of the error. It is presented that the addition of KI keeps the loading more stable and a tiny bit higher compared to unsalted MEA where the loading is not as stable and a bit lower. However, the difference in loading is not significant, thus it can be assumed that the error is relatively small.

Table B.7. Data obtained from the oxidative degradation setup for each parallel on each sample day for the experiment with 30 wt% MEA with 0,5 wt% KI at 60°C. Average alkalinity was calculated as an average of the three parallels on each sample day and is corrected for water loss and loading. Amine remaining was calculated as the percentage of amine left compared to day 0 and it's given with its uncertainty, which was calculated as the standard deviation of the three parallels. The loading was calculated assuming that the alkalinity measured by titration stands for MEA in the solvent. The CO₂ concentration was calculated from the assumed loading from Buvik et al and the titration results with CO₂ from the experiment in this thesis.

30 wt% MEA (aq.) with 0,5 wt% KI							
Day	Total alkalinity w/ CO ₂ [mol/kg]	CO ₂ conc. [g/kg]	Loading ² [mol CO ₂ /mol MEA]	Alkalinity w/o CO ₂ [mol/kg]	Alkalinity corrected [mol/kg]	Avg. alkalinty corrected [mol/kg]	Amine remaining [%]
0	4,53	81,75	0,41	4,90	4,90	4,90	100% ± 0,0%
3a	4,48	82,12	0,42	4,84	4,82		
3b	4,49	85,75	0,43	4,88	4,84	4,83	99% ± 0,3%
3c	4,48	84,42	0,43	4,86	4,83		
7a	4,52	83,57	0,42	4,90	4,83		
7b	4,50	83,27	0,42	4,88	4,79	4,81	98% ± 0,5%
7c	4,51	86,22	0,43	4,90	4,82		
10a	4,53	84,84	0,43	4,92	4,82		
10b	4,57	87,99	0,44	4,97	4,84	4,82	98% ± 0,4%
10c	4,53	85,09	0,43	4,92	4,80		
14a	4,56	83,58	0,42	4,94	4,80		
14b	4,58	84,48	0,42	4,97	4,79	4,79	98% ± 0,3%
14c	4,56	82,76	0,41	4,94	4,77		
17a	4,58	81,66	0,41	4,95	4,78		
17b	4,62	82,85	0,41	5,00	4,78	4,78	98% ± 0,1%
17c	4,59	82,15	0,41	4,97	4,77		
21a	4,59	77,32	0,38	4,94	4,73		
21b	4,68	80,54	0,39	5,06	4,78	4,77	97% ± 0,6%
21c	4,67	80,35	0,39	5,04	4,79		

² The assumption that the loading in the 30 wt% MEA solution with 0.5 wt% KI is equal to the unsalted solution, as explained in section 3.2.3.2, might provide a small error in the results. However, this error should be very small, since the exact same oxidative degradation set up with the same oxidative conditions (temperature, loading, gas flow and gas compositions) was used. In addition, the exact same experimental procedures were also utilized. Hence, the only difference between the execution of the experiments is the addition of KI, which by comparing the loadings presented for 30 wt% MEA with and without KI in the supplementary information given in Buvik et al⁹, might give an indication of the error. It is presented that the addition of KI keeps the loading more stable and a tiny bit higher compared to unsalted MEA where the loading is not as stable and a bit lower. However, the difference in loading is not significant, thus it can be assumed that the error is relatively small.

Table B.8. Data from the HSS analysis for all the experiments presented in this thesis for the initial (day 0) and end solution (day 21). All the values have been corrected for loading and water loss, and the experiments with KI have also been corrected for the addition of this salt. The concentration of KI in each experiment is given in table B.13 in appendix B. The average HSS concentration is calculated as an average of the three parallels in each experiment and it is presented with its uncertainty, which was calculated as the standard deviation of these parallels. The notation n.t is short for not tested. It was assumed that pure amine solutions did not contain any heat stable salts, thus their initial solution is not tested.

<i>Experiment</i>	<i>Day</i>	<i>HSS conc. [mol/kg]</i>	<i>HSS conc. corrected [mol/kg]</i>	<i>Avg. HSS conc. [mol/kg]</i>
<i>Pilot B (30 wt% MEA) w/ 2 wt% KI</i>	0	0,25	0,142	$0,14 \pm 0$
	21a	0,31	0,192	
	21b	0,31	0,193	$0,19 \pm 0,0009$
	21c	0,31	0,192	
<i>Pilot B (30 wt% MEA) w/o salt addition</i>	0	0,17	0,180	$0,18 \pm 0$
	21a	0,33	0,327	
	21b	0,33	0,327	$0,33 \pm 0,004$
	21c	0,33	0,333	
<i>Pilot A (30 wt% MEA) w/ 2 wt% KI</i>	0	0,17	0,06	$0,06 \pm 0$
	21a	0,20	0,086	
	21b	0,19	0,080	$0,09 \pm 0,006$
	21c	0,20	0,092	
<i>Pilot A (30 wt% MEA) w/o salt addition</i>	0	0,05	0,05	$0,05 \pm 0$
	21a	0,18	0,179	
	21b	0,33	0,329	$0,30 \pm 0,12$
	21c	0,40	0,400	
<i>30 wt% AP w/ 2 wt% KI</i>	0	0,11	0,0	0,0
	21a	0,10	-0,013	
	21b	0,11	0,003	$-0,01 \pm 0,006$
	21c	0,10	-0,013	
<i>30 wt% DGA w/ 2 wt% KI</i>	0	n,t	n,t	n,t
	21a	0,10	-0,015	
	21b	0,11	-0,010	$-0,01 \pm 0,003$
	21c	0,10	-0,015	

Table B.8. (Continued).

<i>Experiment</i>	<i>Day</i>	<i>HSS conc [mol/kg]</i>	<i>HSS conc. corrected [mol/kg]</i>	<i>Avg. HSS conc [mol/kg]</i>
<i>30 wt% MEA w/ 0,5 wt% KI</i>	0	n,t	n,t	n,t
	21a	0,04	0,008	0,00 ± 0,003
	21b	0,03	0,002	
	21c	0,03	0,002	

Table B.9. Concentration of total nitrogen in the initial- and end solutions for all the experiments presented in this thesis. The data was obtained from the TN analysis and titration. The values for 30 wt% MEA was obtained from Buvik et al.⁸. All the values obtained for day 21 are calculated as an average of the three parallels in each experiment, and the values are corrected for water loss and loading, Amine conservation and nitrogen loss/conservation were calculated from the initial- and end- result from the titration analysis and the TN analysis, respectively. Uncertainty in amine conservation and nitrogen in degradation products were calculated as standard deviation of the three parallels in each experiment for the titration and TN analysis, respectively. The uncertainty within each parallel is max ±3% (uncertainty of analytical method).

<i>Experiment</i>	<i>TN, day 0 [mol/kg]</i>	<i>TN, day 21 [mol/kg]</i>	<i>Amine conserved, day 21 [%]</i>	<i>N conserved, day 21 [%]</i>	<i>N in deg, products, day 21 [%]</i>	<i>N lost, day 21 [%]</i>
<i>Pilot A (30 wt% MEA) w/ 2 wt% KI</i>	5,65	5,41	95 % ± 0,3%	96 %	0 % ± 1,0%	4 %
<i>Pilot A (30 wt% MEA) w/o salt addition</i>	5,58	4,65	61 % ± 13,9%	83 %	23 % ± 4,8%	17 %
<i>Pilot B (30 wt% MEA) w/ 2 wt% KI</i>	5,77	5,69	93 % ± 0,3%	99 %	6 % ± 1,1%	1 %
<i>Pilot B (30 wt% MEA) w/o salt addition</i>	6,00	5,43	76 % ± 3,6%	91 %	15 % ± 2,3%	9 %
<i>30 wt% AP w/ 2 wt% KI</i>	4,33	4,47	100 % ± 0,5%	103 %	3 % ± 0,4%	-3 %
<i>30 wt% MEA w/o salt addition</i>	5,03	3,99	60 % ± 4%	79 %	20 % ± 4%	21 %

Table B,10. Concentrations of MEA and degradation compounds from the LC-MS analysis after correction of water loss and loading. The initial solutions were also corrected for pure samples by equation (A.4) in appendix A. Uncertainty in the end samples were calculated as the standard deviation of the three parallels the experiments were performed in.

<i>Experiment</i>	<i>MEA</i> [g/kg]	<i>HeGly</i> [g/kg]	<i>HEF</i> [g/kg]	<i>BHEOX</i> [g/kg]	<i>HEA</i> [g/kg]	<i>HEPO</i> [g/kg]	<i>OZD</i> [g/kg]	<i>HEIA</i> [g/kg]	<i>HEHEAA</i> [g/kg]	<i>HEI</i> [g/kg]	<i>HEEDA</i> [g/kg]	<i>MEA urea</i> [g/kg]
<i>Pilot B start</i>	279,501	11,073	1,591	0,106	2,495	18,593	0,028	0,181	0,821	0,525	0,003	2,124
<i>Pilot B, day 21</i>	226,330 ±8	7,551 ± 0,4	8,824 ±0,4	0,819 ± 0,03	3,388 ± 0,2	8,868 ± 0,6	0,207 ± 0,01	0,157 ± 0,01	1,330 ± 0,05	12,322 ± 1	0,005 ± 0,0001	2,322 ± 0,2
<i>Pilot B start, KI</i>	278,711	11,047	1,588	0,106	2,489	18,549	0,028	0,180	0,819	0,523	0,003	2,119
<i>Pilot B, day 21 KI</i>	279,062 ±0,4	12,417 ± 0,7	2,723 ± 0,02	< 0,10 ± < 0,10	2,666 ± 0,07	17,535 ± 0,9	0,224 ± 0,01	0,160 ± 0,001	1,153 ± 0,02	1,465 ± 0,05	< 0,001	2,866 ± 0,05
<i>Pilot A start</i>	286,469	8,063	0,815	< 0,10	0,580	6,753	0,085	0,036	0,553	0,971	0,002	1,445
<i>Pilot A, day 21</i>	172,123 ± 47	1,086 ± 0,2	16,027 ± 3	1,433 ± 0,2	1,326 ± 0,2	1,475 ± 0,7	0,544 ± 0,1	0,028 ± 0,002	0,884 ± 0,2	29,599 ± 11	0,001 ± < 0,001	1,407 ± 0,1

Table B.11. Data obtained from Buvik et al ⁹ on amine loss for different concentration of KI and without the addition of KI in a 30 wt% MEA solution. All experiments were performed at 60°C with the same gas flow and gas composition as in this thesis. The average alkalinity was calculated as the average of the three parallels in each experiment and it is corrected for water loss and loading. Amine remaining was calculated as the percentage of amine left compared to day 0 and it is given along with its uncertainty, which was calculated as the standard deviation between the three parallels in each experiment.

<i>Experiment</i>	<i>Day</i>	<i>Avg. Alkalinity corrected [mol/kg]</i>	<i>Amine remaining [%]</i>
<i>30 wt% MEA w/ 2 wt% KI</i>	0	4,90	100 % ± 0%
	3	4,79	98 % ± 0,7%
	7	4,75	97 % ± 0,4%
	10	4,68	96 % ± 0,7%
	14	4,73	96 % ± 0,3%
	17	4,73	97 % ± 0,3%
	21	4,73	96 % ± 0,5%
<i>30 wt% MEA w/ 1 wt% KI</i>	0	4,90	100 % ± 0%
	3	4,81	98 % ± 0,1%
	7	4,81	98 % ± 0,2%
	10	4,77	97 % ± 0,3%
	14	4,80	98 % ± 0,2%
	17	4,79	98 % ± 0,5%
	21	4,77	97 % ± 0,3%
<i>30 wt% MEA w/ 0.2 wt% KI</i>	0	4,83	100 % ± 0%
	3	4,65	96 % ± 0,2%
	7	4,40	91 % ± 0,7%
	10	4,22	87 % ± 0,8%
	14	3,95	82 % ± 1,9%
	17	3,83	79 % ± 1,4%
	21	3,63	75 % ± 1,6%
<i>30 wt% MEA w/o salt addition</i>	0	4,84	100 % ± 0%
	3	4,63	96 % ± 0,3%
	7	4,24	88 % ± 0,5%
	10	3,91	81 % ± 1,7%
	14	3,49	72 % ± 2,6%
	17	3,22	67 % ± 3,2%
	21	2,89	60 % ± 3,6%

Table B.12. Data obtained from Buvik et al⁸ on amine loss for 30 wt% AP and DGA. All experiments were performed at 60°C with the same gas flow and gas composition as in this thesis. The average alkalinity was calculated as the average of the three parallels in each experiment and it is corrected for water loss and loading. Amine remaining was calculated as the percentage of amine left compared to day 0 and it is given along with its uncertainty, which was calculated as the standard deviation between the three parallels in each experiment.

Experiment	Day	Avg. Alkalinity corrected [mol/kg]	Amine remaining [%]
30 wt% AP	0	4,02	100 % ± 0%
	3	3,98	99 % ± 0,3%
	7	3,90	97 % ± 0,8%
	10	3,85	96 % ± 0,4%
	14	3,79	94 % ± 0,7%
	17	3,74	93 % ± 0,7%
	21	3,67	91 % ± 0,8%
30 wt% DGA	0	2,84	100 % ± 0%
	3	2,80	98 % ± 0,7%
	7	2,68	94 % ± 1,0%
	10	2,55	90 % ± 3,6%
	14	2,44	86 % ± 2,4%
	17	2,32	82 % ± 1,6%
	21	2,28	80 % ± 2,3%

Table B.13. Concentration of KI in the initial solutions of the experiments presented in this thesis. The values are used to correct for the addition of KI in the results from the HSS analysis.

Experiment	KI [mol/kg]
Pilot B (30 wt% MEA) w/ 2 wt% KI	0,12
Pilot A (30 wt% MEA) w/ 2 wt% KI	0,11
30 wt% DGA w/ 2 wt% KI	0,12
30 wt% AP w/ 2 wt% KI	0,11
30 wt% MEA w/ 2 wt% KI	0,11
30 wt% MEA w/ 0,5 wt% KI	0,03

Table B.14. Data obtained from the viscosity measurement for the initial- and end solution for the pre-degraded MEA samples from pilot plant B with and without KI, including the measured loading at day 0 and day 21 obtained from the TIC analysis. The average viscosity and loading are calculated as the average of the three parallels in each experiment and it is given along with its uncertainty. The uncertainty was calculated as the standard deviation between the three parallels in each experiment.

Experiment	Day	Viscosity [mPa*s]	Avg. Viscosity [mPa*s]	Loading [mol CO₂/mol MEA]	Avg. Loading [mol CO₂/mol MEA]
Pilot B w/o salt addition	0	5,27	5,27	0,47	0,47
	21a	4,46		0,45	
	21b	4,69	4,75 ± 0,3	0,44	0,46 ± 0,02
	21c	5,10		0,48	
Pilot B w/ 2 wt% KI	0	5,19	5,19	0,47	0,47
	21a	5,46		0,43	
	21b	5,34	5,43 ± 0,07	0,43	0,43 ± 0
	21c	5,48		0,43	

Table B.15. Data obtained by Buvik et al⁸ from the HSS analysis of 30 wt% AP, DGA and MEA solutions after three weeks of oxidative degradation. The average HSS concentration was calculated as the average of the three parallels in each experiment and it is corrected for water loss and loading. The uncertainty was calculated as the standard deviation between the three parallels in each experiment.

<i>Experiment</i>	<i>avg HSS, day 21 [mol/kg]</i>
<i>AP w/o salt</i>	$0,06 \pm 0,01$
<i>DGA w/o salt</i>	$0,11 \pm 0,02$
<i>MEA w/o salt</i>	$0,33 \pm 0,002$

